

1 **Salmonella enterica** serovar **Typhimurium** ST313 sublineage 2.2
2 has emerged in Malawi with a characteristic gene expression
3 signature and a fitness advantage
4

5
6
7 Benjamin Kumwenda^{1,2,3, #}, Rocío Canals^{2, #}, Alexander V. Predeus^{2, #}, Xiaojun
8 Zhu², Carsten Kröger^{2,4}, Caisey Pulford², Nicolas Wenner², Lizeth Lacharme
9 Lora², Yan Li², Siân V. Owen², Dean Everett⁵, Karsten Hokamp⁶, Robert S.
10 Heyderman^{3,7}, Philip M. Ashton³, Melita A. Gordon^{2,3}, Chisomo L. Msefula^{1,3},
11 Jay C. D. Hinton².

12
13 ¹School of Life Sciences and Health Professions, Kamuzu University of Health Sciences
14 Blantyre, Blantyre, MALAWI

15 ²Institute of Infection, Veterinary & Ecological Sciences, University of Liverpool, Liverpool,
16 UNITED KINGDOM,

17 ³Malawi–Liverpool–Wellcome Programme, Blantyre, MALAWI.

18 ⁴Moyn Institute of Preventive Medicine, Trinity College Dublin, Dublin, IRE.

19 ⁵College of Medicine and Health Sciences, Khalifa University, Abu Dhabi, UAE.

20 ⁶Smurfit Institute of Genetics, School of Genetics and Microbiology, Trinity College Dublin,
21 Dublin, IRE.

22 ⁷Research Department of Infection, Division of Infection & Immunity, University College
23 London, UK.

24
25
26
27
28
29
30
31
32
33
34
35
36
37
38
39
40
41
42
43 **Key words:** transcriptomics, comparative genomics, lineage evolution, gene expression,
44 antibiotic resistance

45
46
47
48
49 #BK, RC and AP contributed equally to this work.

50 **Abstract**

51 Invasive non-typhoidal *Salmonella* (iNTS) disease is a serious bloodstream infection that
52 targets immune-compromised individuals, and causes significant mortality in sub-Saharan
53 Africa. *Salmonella enterica* serovar Typhimurium ST313 causes the majority of iNTS in Malawi,
54 and we performed an intensive comparative genomic analysis of 608 isolates obtained from
55 fever surveillance at the Queen Elizabeth Hospital, Blantyre between 1996 and 2018. We
56 discovered that following the upsurge of the well-characterised *S. Typhimurium* ST313 lineage
57 2 from 1999 onwards, two new multidrug-resistant sublineages designated 2.2 and 2.3,
58 emerged in Malawi in 2006 and 2008, respectively. The majority of *S. Typhimurium* isolates
59 from human bloodstream infections in Malawi now belong to sublineage 2.2 or 2.3. To identify
60 factors that characterised the emergence of the prevalent ST313 sublineage 2.2, we performed
61 genomic and functional analysis of two representative strains, D23580 (lineage 2) and D37712
62 (sublineage 2.2). Comparative genomic analysis showed that the chromosome of ST313
63 lineage 2 and sublineage 2.2 were broadly similar, only differing by 29 SNPs and small indels
64 and a 3kb deletion in the Gifsy-2 prophage region that spanned the *sse*/pseudogene. Lineage
65 2 and sublineage 2.2 have unique plasmid profiles that were verified by long read sequencing.
66 The transcriptome was initially explored in 15 infection-relevant conditions and within
67 macrophages. Differential gene expression was subsequently investigated in depth in the four
68 most important *in vitro* growth conditions. We identified up-regulation of SPI2 genes in non-
69 inducing conditions, and down-regulation of flagellar genes in D37712, compared to D23580.
70 Following phenotypic confirmation of transcriptional differences, we discovered that sublineage
71 2.2 had increased fitness compared with lineage 2 during mixed-growth in minimal media. We
72 speculate that this competitive advantage is contributing to the continuing presence of
73 sublineage 2.2 in Malawi.

74

75 Introduction

76 Non-typhoidal *Salmonella* (NTS) is a major pathogen that threatens people across the world.
77 *Typhimurium* and *Enteritidis* are the two serovars of *Salmonella enterica* that cause the highest
78 levels of self-limiting gastrointestinal disease in Europe, the USA and other high-income
79 countries (Zhang *et al.*, 2003). In the industrialised world, NTS has largely been associated with
80 intensive food production, animal husbandry, and global distribution systems (Majowicz *et al.*,
81 2010). Globally, the most common sequence type of *S. Typhimurium* associated with
82 gastroenteritis is ST19. Diarrhoeal NTS disease (dNTS) is mainly foodborne and poses a
83 significant burden to public health globally, causing approximately 153 million cases and 57,000
84 deaths per annum (Kirk *et al.*, 2015; Chirwa *et al.*, 2023).

85 In contrast, a lethal systemic disease called invasive non-typhoidal Salmonellosis (iNTS) has
86 emerged in recent decades in low- and middle-income countries in sub-Saharan Africa. Cases
87 of iNTS are characterized by bloodstream infections of immune-compromised individuals such
88 as children under five years of age, and HIV-positive adults. Anaemia, malnutrition and malaria
89 are some of the major risk factors (Feasey *et al.*, 2012). In some countries of sub-Saharan
90 Africa, *Salmonella* causes more cases of community-onset bloodstream infections than any
91 other bacterial pathogen (Marchello *et al.*, 2019). In 2017, 535,000 cases of iNTS disease were
92 estimated worldwide, with about 80% of cases and 77,000 deaths occurring in sub-Saharan
93 Africa (Stanaway *et al.*, 2019)

94 Clinically, the treatment of iNTS is complicated by multi-drug (MDR) resistance which limits
95 therapeutic options (Crump *et al.*, 2015). Widespread resistance of iNTS pathogens to first-line
96 drugs such as chloramphenicol, ampicillin and cotrimoxazole has been seen in many countries
97 (Kariuki *et al.*, 2006). This MDR phenotype may be one of the reasons the case fatality rate
98 associated with iNTS is amongst the highest in comparison to any infectious disease (15%)
99 (Marchello *et al.*, 2022) Resistance to second line drugs such as ceftriaxone, ciprofloxacin and
100 azithromycin has been reported in a few African countries (Tack *et al.*, 2020). Clearly, the
101 problem of MDR *Salmonella* must be addressed urgently (Gilchrist and MacLennan, 2019).

102 The African iNTS epidemic is mainly caused by two *Salmonella* pathovariants, *S. Typhimurium*
103 sequence type 313 (ST313) and specific clades of *S. Enteritidis* (Kingsley *et al.*, 2009; Okoro
104 *et al.*, 2012; Feasey *et al.*, 2016). *S. Typhimurium* ST313 is responsible for about two-thirds of
105 clinical iNTS cases that have been reported in Africa (Gilchrist and MacLennan, 2019).

106 It is not certain how these pathogens are transmitted, but there is increasing evidence from
107 case-control studies that ST313 strains are human-associated but not animal-associated within
108 households (Post *et al.*, 2019; Koolman *et al.*, 2022). A recent summary concludes that the
109 available data are consistent with the person-to-person transmission hypothesis for iNTS
110 disease (Chirwa *et al.*, 2023). Global efforts to combat iNTS infections are currently focused on
111 vaccine development which is currently progressing to clinical trials (Piccini and Montomoli,
112 2020).

113 Since 1998, continuous sentinel surveillance for fever and bloodstream infections among adults
114 and children has been undertaken at Queen Elizabeth Central Hospital (QECH). This tertiary
115 referral hospital in Blantyre, Malawi, serves an urban population of about 920,000 with a high
116 incidence of malaria, HIV and malnutrition (Musicha *et al.*, 2017). Following blood-culture of
117 samples collected from patients of all ages presenting with fever, whole genome sequencing
118 identified the ST313 variant of *S. Typhimurium* (Kingsley *et al.*, 2009). Phylogenetic analysis
119 revealed that the chloramphenicol-sensitive ST313 lineage 1 was clonally-replaced in Malawi
120 by the chloramphenicol-resistant lineage 2 (Okoro *et al.*, 2012). More recently, a ST313
121 sublineage II.1 (2.1) emerged from lineage 2 in Democratic Republic of Congo (DRC) in Central
122 Africa. Sublineage 2.1 had altered phenotypic properties including biofilm formation and
123 metabolic capacity and resistance to azithromycin (Van Puyvelde *et al.*, 2019).

124 An initial suggestion that ST313 lineage 2 was undergoing evolutionary change in East Africa
125 came from a small study that identified seven *S. Typhimurium* ST313 Malawian isolates, dated
126 between 2006 and 2008, that differed from lineage 2 by 22 core-genome single nucleotide
127 polymorphisms (SNPs) (Msefula *et al.*, 2012).

128 To begin to examine the evolutionary trajectory of *S. Typhimurium* in Malawi at a large scale,
129 we conducted a comparative genomic analysis study focused on 680 isolates dating between
130 1998 and 2018 (Pulford *et al.*, 2021). We previously confirmed that ST313 lineage 1 (L1) was
131 replaced by lineage 2 (here designated L2.0), and discovered an antibiotic-sensitive lineage 3
132 (L3) that emerged in 2016 (Pulford *et al.*, 2021).

133 We performed a more intensive phylogenetic analysis of the same collection of *S. Typhimurium*
134 ST313 isolates, most of which caused bloodstream infections in Malawi over two decades. We
135 discovered two novel sublineages named 2.2 (L2.2) and 2.3 (L2.3) that have been replacing
136 L2.0 since 2006.

137 Here we present a comprehensive comparative genomic analysis of the most prevalent ST313
138 L2.2 sublineage, and report the results of a functional genomic approach that identified key
139 phenotypic characteristics that distinguish L2.2 from L2.0.

140

141 **Results**

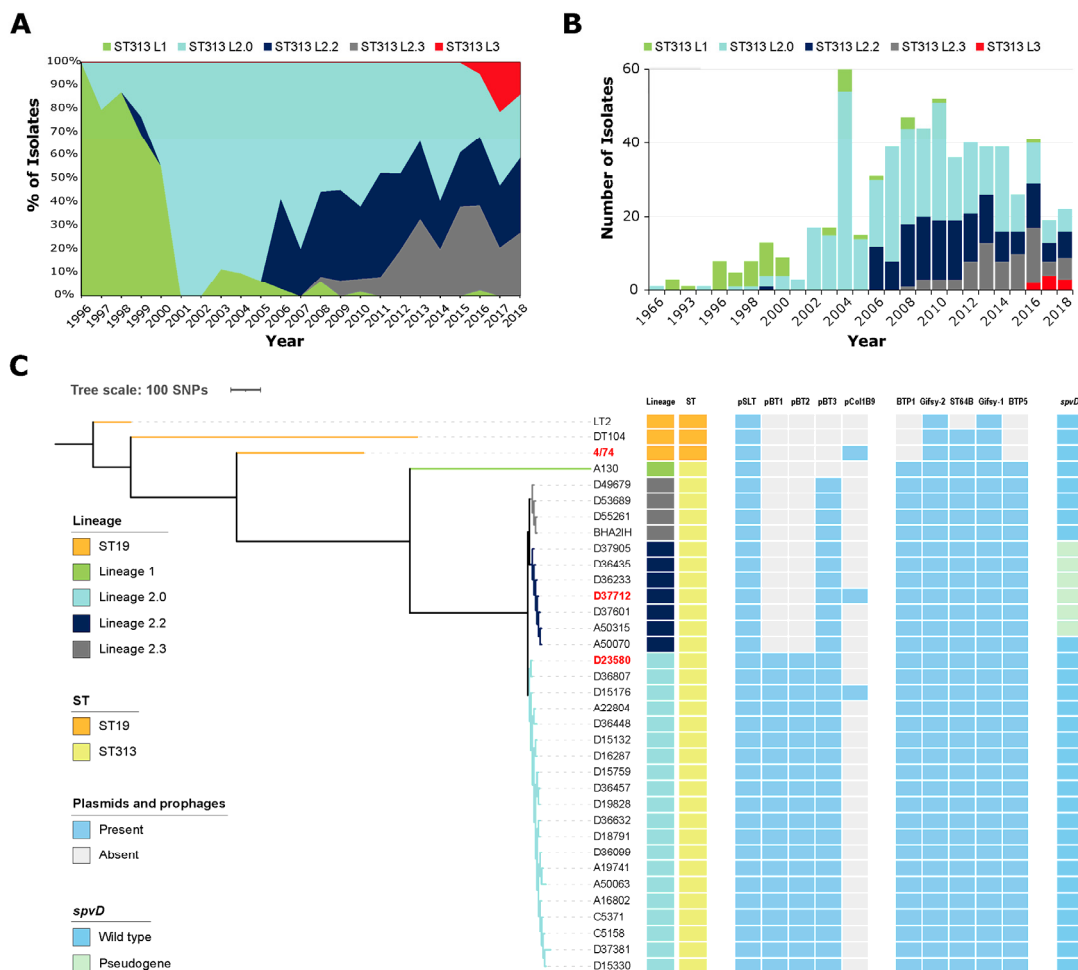
142 **Identification of *S. Typhimurium* ST313 sublineages 2.2 and 2.3 in Malawi**

143 The *S. Typhimurium* ST313 L2 (Lineage II) was originally identified as the major cause of iNTS
144 cases across sub-Saharan Africa in the early 2000's (Kingsley *et al.*, 2009; Okoro *et al.*, 2012)
145 (Okoro *et al.*, 2015). Subsequently, an azithromycin-resistant variant of *S. Typhimurium* ST313
146 was found in a single country, the Democratic Republic of Congo between 2008 and 2016, and
147 was designated sublineage L2.1 (Van Puyvelde *et al.*, 2019).

148 To investigate the evolutionary dynamics of *S. Typhimurium* ST313 L2 in Malawi over a 22 year
149 period, we focused on the large collection of 8,000 *S. Typhimurium* isolates derived from

150 bloodstream infection in hospitalised patients at the Queen Elizabeth Central Hospital, Blantyre,
151 Malawi (Feasey *et al.*, 2015). The collection was assembled by the Malawi–Liverpool–
152 Wellcome Trust Clinical Research Programme (MLW) between 1996 and 2018; the precise
153 annual numbers of isolates are shown in Fig 1B. A random sub-sampling strategy was used to
154 select 608 isolates selected for whole-genome sequencing which included 549 *S. Typhimurium*
155 ST313 isolates (Pulford *et al.*, 2021).

156



157

158 **Fig 1. Emergence of *S. Typhimurium* ST313 sublineages L2.2 and L2.3 in Malawi.** (A) Evolutionary dynamics of *S. Typhimurium* lineages in Blantyre, Malawi from 1996 to 2018. The 159 genomes of 549 *S. Typhimurium* ST313 isolates from bacteraemic patients at the Queen 160 Elizabeth Hospital in Blantyre, Malawi were used for this analysis. The proportions of the five 161 lineages/sublineages are shown. (B) The total number of isolates of each lineage/sublineage 162 per year. (C) Phylogenetic comparison between representative strains of *S. Typhimurium* ST19 163 and four ST313 lineages/sublineages (L1, L2.0, L2.2, L2.3) showing the presence and absence 164 of plasmids, prophages and the *spvD* pseudogene. The complete phylogenetic analysis of 707 165 *S. Typhimurium* genomes is shown in Fig.S1. 166

167

168 Here, we used a core-gene SNP-based maximum likelihood (ML) phylogenetic tree to 169 investigate the population structure of *S. Typhimurium* ST313 L2.0 in more detail (Fig. S1). As 170 well as identifying members of the antibiotic-sensitive lineage 3 that we reported previously

171 (Pulford *et al.*, 2021), we discovered that ST313 L2 could be split into three phylogenetically-
172 distinct sublineages that differed by 39 SNPs. The *S. Typhimurium* ST313 L2 reference strain
173 D23580 (Kingsley *et al.*, 2009) belonged to the first sublineage, which we have now designated
174 as ST313 L2.0 (Fig 1C). As ST313 sublineage L2.1 has been defined previously (Van Puyvelde
175 *et al.*, 2019), the new sublineages were designated as L2.2 and L2.3, and belonged to different
176 hierBAPS level 2 clusters (Fig 1C and Fig S1). We identified 151 L2.2 isolates and 74 L2.3
177 isolates, against a backdrop of 350 L2.0 isolates.

178 In Blantyre, Malawi, *S. Typhimurium* ST313 L2.2 was first detected in 2006, and L2.3 was
179 initially observed in 2008 (Fig. 1A. Both L2.2 and L2.3 increased in prevalence at the Queen
180 Elizabeth Central Hospital in Blantyre in subsequent years. By 2018, L2.2 and L2.3 had largely
181 replaced L2.0 (Fig 1A-B). Our published Bayesian (BEAST) analysis (Pulford *et al.*, 2021)
182 estimated that the Most Recent Common Ancestor (MRCA) of ST313 lineage 2 dates back to
183 1948 (95% HPD = 1929-1959).

184 To understand the accessory gene complement of L2.2 and L2.3, we compared the genomes
185 of seven L2.2 isolates and four L2.3 isolates with 17 L2.0 isolates, ST313 L1 and ST19 (Fig
186 1C, Table S1). *S. Typhimurium* strain D23580 is the representative strain of L2.0 (Kingsley *et*
187 *al.*, 2009), for which we previously used long-read sequencing and other approaches to
188 thoroughly characterise the chromosome and the plasmid complement (Canals *et al.*, 2019b).

189

190 **Antimicrobial Resistance**

191 AMR variants of *S. Typhimurium* with resistance to ampicillin and cotrimoxazole were detected
192 at an early stage of the iNTS epidemic, from 1997 onwards (Gordon *et al.*, 2008). Multidrug-
193 resistant variants of *S. Typhimurium* ST313 that were no longer susceptible to chloramphenicol,
194 ampicillin and cotrimoxazole subsequently emerged in Malawi (Gordon *et al.*, 2008) and have
195 been reported elsewhere in sub-Saharan Africa by the GEMS study (Kasumba *et al.*, 2021).
196 The *S. Typhimurium* ST313 L2.0, L2.2 and L2.3 isolates shared the same MDR profiles
197 (resistance to chloramphenicol, ampicillin and cotrimoxazole), and carried identical IS21-AMR
198 gene cassettes within the pSLT-BT plasmid.

199

200 **Comparative genomics of *S. Typhimurium* ST313 sublineage 2.2**

201 Because *S. Typhimurium* ST313 L2.2 was the predominant novel sublineage in Blantyre,
202 Malawi, we focused on L2.2 for the remainder of this study. We used the phylogeny (Fig 1C) to
203 select strain D37712 as a representative isolate of L2.2. D37712 was isolated from the blood
204 of an HIV-positive Malawian male child and has been deposited in the National Collection of
205 Type Cultures (NCTC). The initial genome sequence of D37712 was obtained in 2012 with
206 Illumina technology, an assembly that comprised 27 individual contigs (Msefula *et al.*, 2012).
207 To generate a reference-quality genome, we resequenced D37712 with both long-read PacBio
208 and Illumina short-read technologies. Our hybrid strategy generated a complete genome

209 assembly that included one circular chromosome and three plasmids (see Materials & Methods;
210 GenBank CP060165, CP060166, CP060167 and CP060168). This high-quality genome
211 sequence allowed us to conduct a detailed comparative genomic analysis of L2.2 strain D37712
212 with L2.0 strain D23580 (accession number FN424405), summarised in Fig. 2 and Table S2.

213 Overall, the two strains contain a similar number of genes. The D37712 and D23580 genomes
214 shared 5,016 orthologous genes, including 4,729 protein-coding genes and pseudogenes as
215 well as the 287 small RNA (sRNA) genes that we identified previously. The D23580 annotation
216 contains 4,823 protein-coding and pseudogenes and 287 sRNAs (Canals *et al.*, 2019b), while
217 D37712 contains 4,821 protein-coding and pseudogenes and 287 sRNAs.

218 **Overview of D23580 and D37712 genomes**

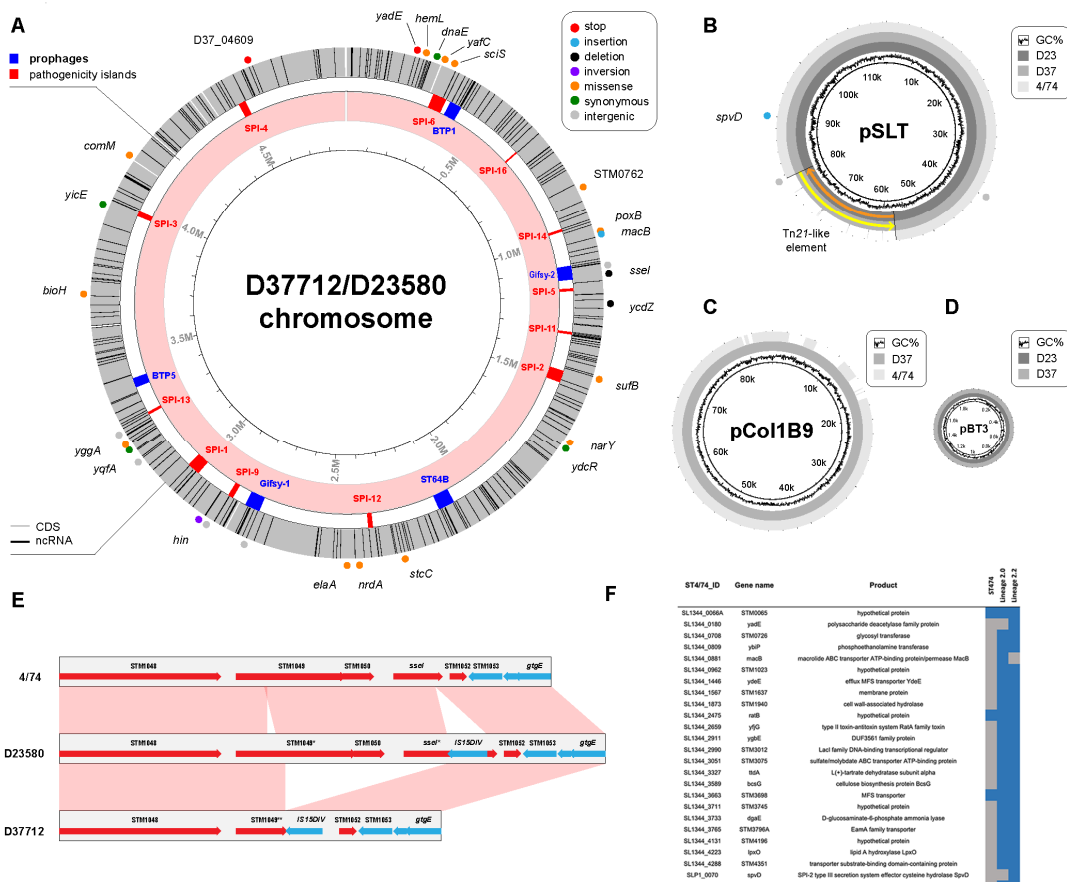
219 The chromosomes of D23580 and D37712 are 4,879,402 and 4,876,060 bp, respectively, and
220 similar in size to other *S. Typhimurium* genomes (Kingsley *et al.*, 2009; Branchu *et al.*, 2018).
221 The D23580 and D37712 strains share a similar prophage profile, with both strains carrying
222 five prophages (BTP1, Gifsy-2, ST64B, Gifsy-1, and BTP5) which were located at the same
223 positions on the chromosome. Previously, we have established that just one of these
224 prophages, BTP1, is functional (Owen *et al.*, 2017). The BTP1 prophage of D23580 encodes
225 the novel BstA phage defence system (Owen *et al.*, 2021) and a particularly high level of viable
226 BTP1 phages is produced by spontaneous induction (Owen *et al.*, 2017).

227 **Comparison of D23580 and D37712 chromosomes**

228 The detailed genomic comparison of D37712 with D23580 showed that the two genomes were
229 remarkably similar. Overall, the only differences between the genomes of the L2.0 and L2.2
230 strains were 26 chromosomal SNPs and small indels, plus one large deletion, and an inversion
231 of the *hin* switch. In-depth annotation of the nucleotide variants identified 3 putative loss-of-
232 function mutations (2 stop mutations, 1 frameshift insertion), 1 disruptive in-frame deletion, 4
233 synonymous mutations, 13 missense mutations, and 5 intergenic variants, summarised in Fig
234 2A.

235 The 3,358 bp-long deletion of a Gifsy-2 prophage-associated region that spanned the *sseI*
236 pseudogene of D23580 removed two coding sequences (STM1050-51; STMMW_10611-
237 STMMW_10631), and substantially truncated the STM1049 (STMMW_10601) gene (Fig 2E).
238 The *sseI* gene encodes a cysteine hydrolase effector protein that modulates the directional
239 migration of dendritic cells during systemic infection (Brink *et al.*, 2018). In strain D23580, the
240 insertion of a transposable element IS15DEV inactivated the *sseI* gene (Kingsley *et al.*, 2009)
241 causing increased dendritic cell-mediated dissemination of strain D23580 during infection
242 (Carden *et al.*, 2017). To confirm that the 3,358 bp deletion removed the *sseI* gene from the
243 chromosome of strain D37712, we used an independent PCR-based approach (Fig S2).

244



245

246

247 **Fig 2. Key genetic similarities and differences between the chromosome and plasmid**
248 **profiles of D23580 (lineage 2) and D37712 (L2.2). (A)** A comparison of the D23580 (L2.0)
249 and D37712 (L2.2) chromosomes. The dots around the chromosome are different kinds of
250 SNPs identified. Phages and *Salmonella* pathogenicity islands are shown in blue and red
251 respectively. **(B)** Plasmid profile of D37712 versus D23580. The pSLT-BT virulence plasmid is
252 present in both D37712 and D23580, and carries the Tn-21 transposable element; **(C)** pCol1B9
253 is present in D37712 and absent from D23580 **(D)** pBT3 is present in both D37712 and D23580.
254 **(E)** Absence of sseI gene and the STM1050 coding sequence in L2.2 (D37712), as compared
255 to *S. Typhimurium* ST19 4/74 and *S. Typhimurium* ST313 L2.0 (D23580). **(F)** List of
256 pseudogenes in D37712 and D23580, with reference to 4/74. The colour blue means
257 pseudogene/disrupted gene while grey indicates functional genes. *macB* is a pseudogene in
258 D23580 (L2.0) but not in L2.2, while *spvD* is a pseudogene in L2.2 but not in L2.0. All L2.2
259 strains share similar pseudogenes.

260

261 Comparison of D23580 and D37712 plasmids

262 ST313 L2.0 strain D23580 carries four plasmids, pSLT-BT, pBT1, pBT2 and pBT3 (Kingsley et
263 al., 2009). In contrast, ST313 L2.2 carried a distinct plasmid complement (Fig 1C, Fig. 2BCD).
264 In summary, strain D37712 carried pSLT-BT, pBT2 and pCol1B9 as detailed below. Both
265 strains had a variant of the pSLT-BT virulence plasmid (Kingsley et al., 2009) that contains a
266 Tn21-like transposable element with five antibiotic resistance genes. The D37712 version of
267 pSLT-BT is similar to that of D23580, with two important differences (Fig 2B). Firstly, the Tn21-
268 like element is inserted in the opposite direction with regards to the rest of the plasmid,

269 suggesting that the transposable element remains active. Secondly, three nucleotide variants
270 were identified in the pSLT-BT variant, two deletions in noncoding regions, and one frameshift
271 insertion that generates a pseudogene of *spvD*. The SpvD effector protein, a cysteine protease,
272 is translocated by the SPI2 type 3 secretion system and suppresses the NF- κ B-mediated pro-
273 inflammatory immune response and contributes to virulence in mice (Grabe *et al.*, 2016).

274

275 Plasmid pCol1B9 was of particular interest because it was absent from D23580, but is present
276 in *S. Typhimurium* ST19 strain 4/74 (Richardson *et al.*, 2011). 4/74 is the parent of the *S.*
277 *Typhimurium* SL1344 strain that has been used extensively for the study of *S. Typhimurium*
278 pathogenesis and gene regulation since 1986 (Kröger *et al.*, 2012; Rankin & Taylor, 1966).
279 Our annotation of the pCol1B9 plasmid included 95 distinct protein-coding genes, while the
280 previously published annotation of pCol1B9^{4/74} assigned 101 protein-coding genes. Some of
281 these represent annotation discrepancies, while others represent true genetic differences (Fig.
282 S3). Upon careful examination, 14 genes were unique to pCol1B9^{D37712}, while 20 were unique
283 to pCol1B9^{4/74}. There were 81 genes carried by both plasmids. Interestingly, pCol1B9^{D37712}
284 lacked the colicin toxin-antitoxin system that both gave pCol1B9 its name, and provides
285 *Salmonella* with a competitive advantage in the gut (Nedialkova *et al.*, 2014). The pCol1B9^{D37712}
286 plasmid carried a locus that was absent from pCol1B9^{4/74}, namely the *impC-umuCD* operon
287 (Fig. S3) which encodes the error-prone DNA polymerase V responsible for the increased
288 mutation rate linked to the SOS stress response in *E. coli* (Sikand *et al.*, 2021).

289 An 85 kb plasmid carried by D23580, pBT1, was previously shown by our laboratory to play an
290 important role in *Salmonella* biology by encoding an orthologous *cysS* gene responsible for
291 expressing the essential cysteinyl tRNA-synthetase enzyme (Canals *et al.*, 2019b). This pBT1
292 plasmid was completely absent from D37712, and from all isolates of sublineage L2.2 that were
293 examined (Fig. 1C).

294

295 Comparison of pseudogene status of D23580 and D37712

296 Our comparative genomic analysis focused on the pseudogenes found in strains 4/74, D23580,
297 and D37712 (Fig 2F, Table S3). The pseudogenisation of several D23580 genes, compared
298 with strain 4/74, have been linked to the invasive phenotype of African *Salmonella* ST313
299 (Kingsley *et al.*, 2009). We found that the pseudogene complement of D23580 was largely
300 conserved in D37712. We have recently reported the role of the MacAB-TolC macrolide efflux
301 pump in the virulence of *S. Typhimurium* ST313, and showed experimentally that *macB* was
302 an inactive pseudogene in D23580 (Honeycutt *et al.*, 2020). Interestingly, the *macB* gene is
303 functional in D37712. Compared with D23580, three additional D37712 genes were
304 pseudogenised (*spvD*, *yadE*, and STMMW_42692).

305 Overall the chromosomes of ST313 lineage 2 and sublineage 2.2 were highly-conserved and
306 differed by just 29 SNPs/ small indels, and a 3kb deletion in the Gifsy-2 prophage region. The

307 ST313 lineage 2 and sublineage 2.2 have distinct plasmid profiles.

308 **Transcriptional landscape of *S. Typhimurium* ST313 sublineage L2.2**

309 Previously, we characterized the primary transcriptome of two other *S. Typhimurium* strains,
310 4/74 and D23580, using a combination of multi-condition RNA-seq and differential RNA-seq
311 (dRNA-seq) techniques (Canals *et al.*, 2019b; Kröger *et al.*, 2013). To identify the transcriptional
312 start sites (TSS) of strain D37712, we analysed a pooled sample containing RNA from 15 *in*
313 *vitro* conditions by dRNA-seq and RNA-seq as detailed previously (Kröger *et al.*, 2013). The
314 high similarity between the D23580 and D37712 chromosomes allowed us to map the curated
315 set of TSS that were previously defined for D23580 (Hammarlof *et al.*, 2018) onto a combined
316 D37712/D23580 reference genome. To allow individual TSS to be examined in particular
317 chromosomal or plasmid regions, data from both the dRNA-seq and pooled RNA-seq
318 experiments can be visualised in our online genome browser
319 (http://hintonlab.com/jbrowse/index.html?data=Combo_D37/data).

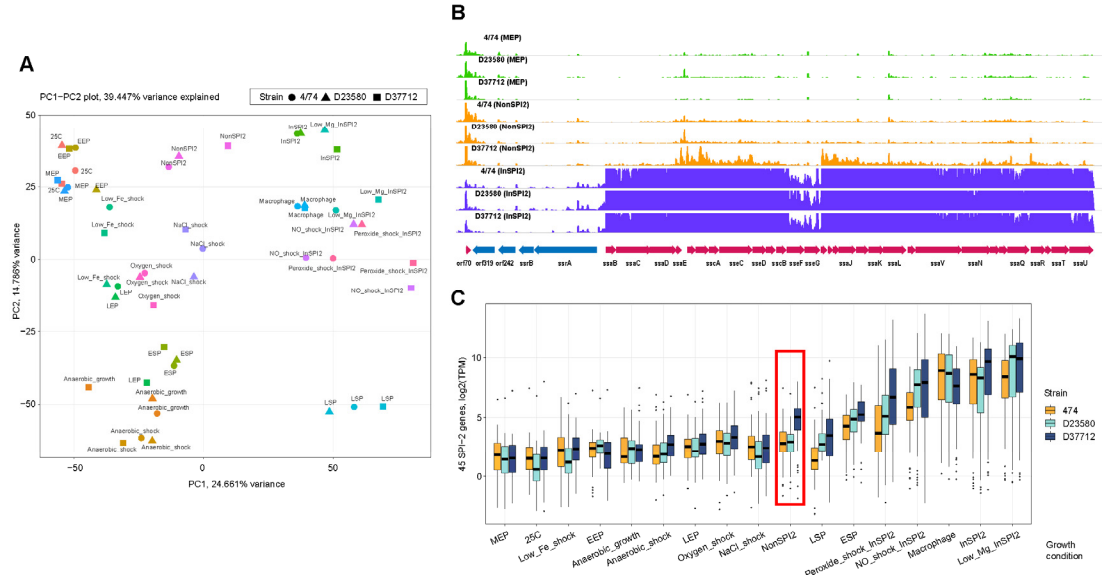
320 **Preliminary gene expression profiling of *S. Typhimurium* ST313 sublineage
321 L2.2**

322 Given the high level of similarity between the genomes of L2.2 and L2.0, we went on to identify
323 differences at the transcriptional level. We performed a multi-condition RNA-seq-based
324 transcriptomic analysis of gene expression profiles of L2.2 strain D37712 without biological
325 replicates.

326 This comparative transcriptomic screen was based on our published approach (Canals *et al.*,
327 2019b). Specifically, we used 15 individual infection-relevant *in vitro* conditions (Kröger *et al.*,
328 2013) and did intra-macrophage transcriptome profiling using the protocol previously
329 established for *S. Typhimurium* ST19 (Srikumar *et al.*, 2015). The RNA-seq samples were
330 mapped to a combined reference genome, which included the annotated D23580 chromosome
331 (Canals *et al.*, 2019b), as well as all the plasmids described earlier (pSLT-BT, pBT1, pBT3 and
332 pCol1B9; see Methods). The initial RNA-seq assessment (detailed in Methods) involved 2-4M
333 non-rRNA/tRNA reads per sample, allowing gene signatures specific for each *in vitro* condition
334 to be identified. Although single replicate RNA-seq experiments of this type cannot be used for
335 statistically-robust differential gene expression analysis, they do provide a useful screening
336 approach for identifying growth conditions to be used for follow-up experiments. The individual
337 RNA-seq experiments showed broad condition-specific similarities in gene expression between
338 strains 4/74, D37712, and D23580 (Fig 3A). The gene expression values from each profiled
339 condition are available as raw counts and TPMs in Tables S4 and S5.

340 To select the ideal environmental conditions to use for subsequent experiments, we assessed
341 the expression profiles of known *Salmonella* pathogenicity islands which were broadly similar
342 in strains D37712, and D23580. Although the expression profile of the SPI2 pathogenicity island
343 was broadly similar between D37712, D23580 and 4/74 in most growth conditions, the SPI2
344 genes of D37712 were highly up-regulated in a single growth condition, NonSPI2 (Fig. 3B-C).
345 NonSPI2 is a minimal medium with a neutral pH and a relatively high level of phosphate, in

346 which *S. Typhimurium* does not usually express the SPI2 pathogenicity island (Löber *et al.*,
347 2006; Kröger *et al.*, 2013). This intriguing observation prompted us to perform the more
348 discriminating set of transcriptomic experiments described below.

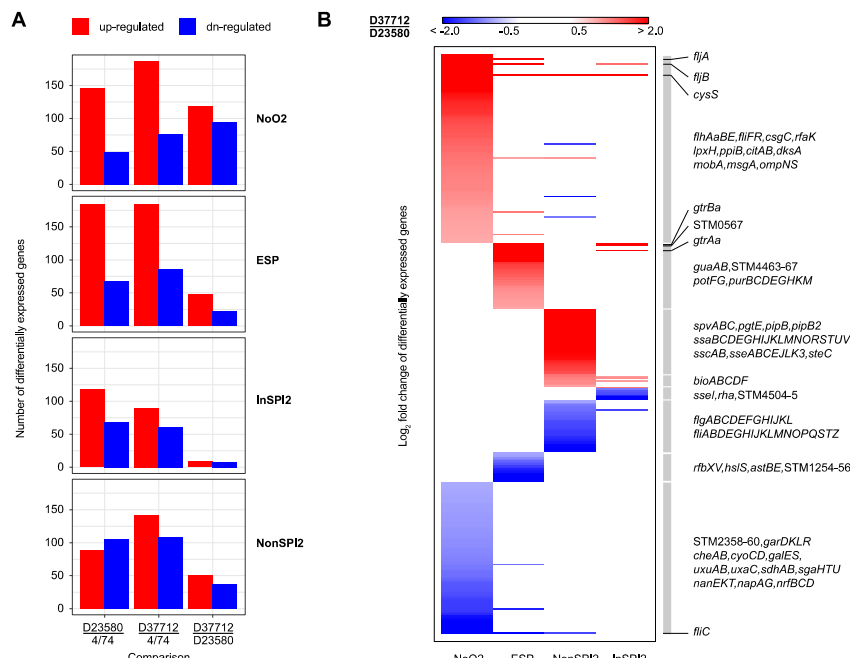


349
350 **Fig 3. General comparison of expression profiles of strains 4/74, D23580, and D37712**
351 **under 17 different *in vitro* conditions.** (A) Principal component analysis (PCA) plot of the
352 individual RNA-seq samples, indicating the overall similarity in gene expression between the
353 three strains. The 17 growth conditions have been defined previously (Kröger *et al.*, 2013). (B)
354 Visualization of SPI-2 pathogenicity island expression with the Jbrowse genomic browser,
355 under mid-exponential phase (MEP), InSPI2, and NonSPI2 *in vitro* conditions. (C) Boxplot
356 visualization of SPI-2 gene expression under mid-exponential phase (MEP), InSPI2, and
357 NonSPI2 *in vitro* conditions. The elevated expression of SPI-2 genes in strain D37712 cultured
358 under NonSPI2 conditions is highlighted in a red box.

359

360 **Differential gene expression analysis of *S. Typhimurium* D37712 versus D23580 in four**
361 ***in vitro* conditions with multiple biological replicates**

362 To define the transcriptional signature of strain D37712 more accurately, we generated RNA-
363 seq data from D37712 grown in four *in vitro* conditions that stimulate expression of the majority
364 of virulence genes: ESP, anaerobic growth, NonSPI2 and InSPI2, with multiple (3-4) biological
365 replicates. We compared the results with our published transcriptomic data for *S. Typhimurium*
366 strains 4/74 and D23580 (Canals *et al.*, 2019b; Kröger *et al.*, 2013). Differential expression
367 analysis with DEseq2, with conservative cut-offs (fold change ≥ 2 , FDR ≤ 0.001), showed that
368 the gene expression profiles of D37712 and D23580 were broadly similar, and shared key
369 differences to the transcriptional profile of strain 4/74 under each of the four *in vitro* conditions
370 (Fig 4A). The differential expression results are summarized in Table S6.



371

372 **Fig 4. Differential gene expression of *S. Typhimurium* 4/74, D37712, and D23580 under 4**
373 **in vitro conditions.** (A) Boxplots indicating the number of differentially-expressed genes
374 identified in the following *in vitro* growth conditions: early stationary phase, ESP; anaerobic
375 growth, NoO2; SPI-2 inducing medium, InSPI2; SPI-2 non-inducing minimal medium, NonSPI2.
376 Multiple (3 to 5) biological replicates were used for comparison. DESeq2 was used for
377 differential analysis; only genes with $|\log_2\text{FC}| \geq 1$ and with adjusted $p\text{-value} \leq 0.001$ were
378 retained. (B) Heatmap of the genes differentially expressed between D23580 and D37712.
379 Functional groups and operons of interest are highlighted on the right of Panel B.

380

381 We specifically investigated transcription of the *pgtE* gene, which encodes the outer- membrane
382 protease previously linked to the ability of African *Salmonella* ST313 to resist human serum
383 killing (Hammarlöf et al., 2018). Compared to 4/74, the *pgtE* gene of both the D23580 and
384 D37712 strains showed a similar pattern of up-regulation by a factor of 7 to 18 across all
385 conditions. This finding is consistent with the fact that D37712 carries the same T nucleotide in
386 the -10 region of the *pgtE* promoter that is responsible for increased expression of the *pgtE*
387 transcript in strain D23580 (Hammarlöf et al., 2018).

388 The majority (92%) of 4,729 orthologous coding genes of both D37712 and D23580 were
389 expressed at similar levels. We identified a total of 364 genes that were differentially expressed
390 in at least one growth condition between D37712 and D23580 as follows: ESP (69 differentially-
391 expressed genes), anaerobic growth (214 differentially-expressed genes), NonSPI2 (88
392 differentially-expressed genes) and InSPI2 (17 differentially-expressed genes; Fig 4B).

393 Overall, the differentially expressed genes that distinguished D37712 from D23580 were seen
394 in a single growth condition and included flagellar genes (down-regulated), SPI2-associated
395 genes (up-regulated), and genes involved in general and anaerobic metabolism (down-
396 regulated).

397 The SPI2 pathogenicity island genes play a key role in the intracellular replication of *S.*
398 *Typhimurium*, and encode the type III secretion system that is responsible for translocation of
399 key effector proteins into mammalian cells (Jennings *et al.*, 2017). The RNA-seq data showed
400 that SPI2 genes were expressed at similarly high levels in both D37712 and D23580 strains
401 following induction (InSPI2 media; Fig 4B), and confirmed that the key SPI2 expression
402 difference was only seen in strain D37712 under non-inducing growth conditions (NonSPI2
403 media). It is important to put this differential SPI2 expression into context. D37712 expresses
404 SPI2 genes at about a 10-fold higher level than D23580 during growth in non-inducing NonSPI2
405 media, but the actual level of expression was 20-fold less than the level stimulated by growth
406 in SPI2-inducing conditions (InSPI2 medium).

407 The up-regulation of *fliA* and *fliB* and the down-regulation of *fliC* in D37712, compared to
408 D23580 in all four growth conditions likely reflects the opposite orientation of the *hin* switch in
409 the D37712 genome compared to D23580. This type of *hin* inversion occurs frequently in *S.*
410 *Typhimurium* (Johnson and Simon, 1985).

411 Another gene that was up-regulated in D37712 across all profiled conditions was the
412 chromosomally-encoded *cysS^{chr}*, that encodes cysteine-tRNA synthetase. Previously, we
413 reported that transcription of the *cysS^{chr}* of strain D23580 was uniformly down-regulated
414 compared to 4/74, a defect that was compensated by the presence of a pBT1 plasmid-encoded
415 cysteine-tRNA synthetase (Canals *et al.*, 2019a). Increased expression of the chromosomal
416 *cysS* gene in D37712 was consistent with the absence of the pBT1 plasmid. Our comparative
417 transcriptomic analysis showed that expression levels of *cysS* were similar in D37712 and 4/74
418 under all growth conditions.

419 Numerous virulence genes and operons were differentially expressed between D23580 and
420 D37712. The SPI-16-associated *gtrABCa* operon (STM0557, STM0558, STM0559) is
421 responsible for adding glucose residues to the O-antigen subunits of LPS that enhance the
422 long-term colonisation of the mammalian gastrointestinal tract by *S. Typhimurium* ST19
423 (Bogomolnaya *et al.*, 2008). We found that the *gtrABCa* genes were significantly up-regulated
424 in several conditions in D37712, compared to both D23580 and 4/74.

425 The *spvABCD* operon of D37712 was up-regulated under non-SPI2-inducing growth
426 conditions, compared to D23580. A signature pseudogene of ST313 L2.2 is the frameshift
427 insertion in the *spvD* gene that generates a truncated version of the SpvD protein. The H199I
428 mutation at position 199 and the associated 17 amino acid truncation is predicted to ablate the
429 activity of the SpvD cysteine protease (Grabe *et al.*, 2016). The functional consequences of the
430 *spvD* variant of ST313 L2.2 strain D37712 and the up-regulation of the *spvABCD* operon remain
431 to be established experimentally.

432 **The SalComD37712 community transcriptional data resource**

433 To allow scientists to gain their own biological insights from analysis of this rich transcriptomic
434 dataset, the transcriptomic and gene expression data generated in this study are presented
435 online in a new community resource, [SalComD37712](#). The data resource shows the expression

436 levels of all D37712 coding and non-coding genes, including both chromosomal and plasmid-
437 encoded transcripts. The SalComD37712 website complements our existing SalComD23580
438 (<https://tinyurl.com/SalComD23580>) resource, and adds an inter-strain comparison of gene
439 expression profiles between D37712 and D23580 as well as normalized gene expression
440 values (TPM), using an intuitive heat map-based approach. [SalComD37712](#) included our
441 published RNA-seq data (Canals *et al.*, 2019b), re-analysed with an updated bioinformatic
442 pipeline and a combined reference genome (see Methods). This online resource facilitates the
443 intuitive interrogation of transcriptomic data as described previously (Perez-Sepulveda and
444 Hinton, 2018).

445 Additionally, we generated a unified genome-level browser that provides access to the *S.*
446 *Typhimurium* L2.2 D37712 transcriptome, in the context of our previously published RNA-seq
447 data for the L2.0 strain D23580 and the ST19 strain 4/74. This novel “combo” browser is
448 available at http://hintonlab.com/jbrowse/index.html?data=Combo_D37/data.

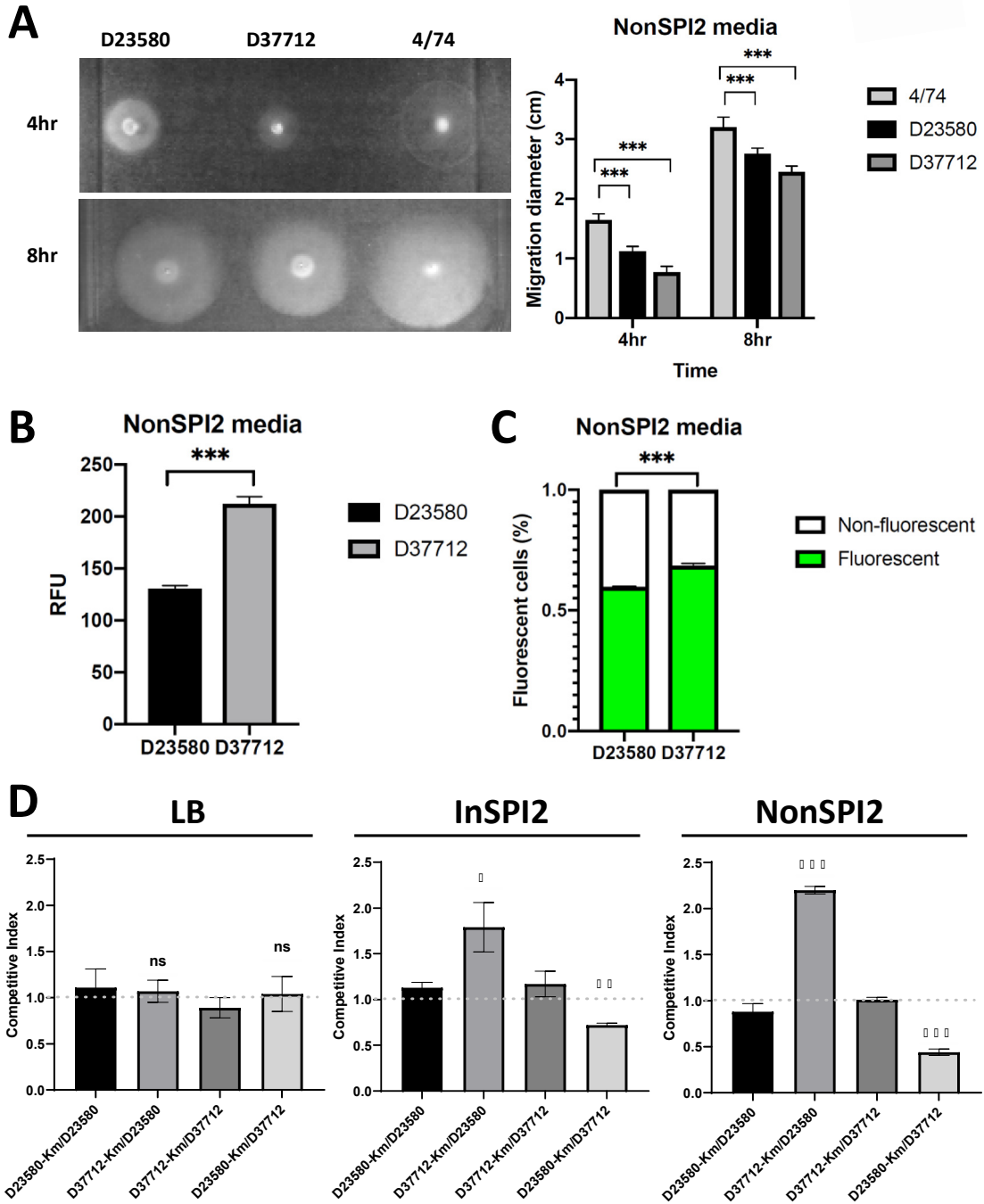
449

450 **Identification of phenotypes that distinguish ST313 sublineage L2.2 from L2.0.**

451 To explore the phenotypic impact of the transcriptomic signature of L2.2 (D37712), we
452 performed a series of motility experiments, fluorescence-based gene expression experiments
453 and mixed-growth assays.

454 D33712 showed a significantly decreased level of motility on NonSPI2 minimal media,
455 compared with both the ST19 strain 4/74 and the L2 D23580 strain (Fig. 5A). This finding was
456 consistent with the transcriptomic data, which showed down-regulation of D37712 flagellar
457 genes compared with D23580 in the NonSPI2 condition (Fig. 4). In contrast, no differential
458 expression of flagellar genes was seen between D33712 and D23580 in the InSPI2 growth
459 condition (Fig. 4). The decreased motility phenotype may be linked to the inversion of the *hin*
460 element detailed above. The flagella system encodes a distinct type III secretion apparatus
461 responsible for the dual functions of bacterial motility and activation of the mammalian innate
462 immune system via TLR5 (Lai *et al.*, 2013).

463 A key transcriptomic finding for strain D33712 was the expression of SPI2 genes during growth
464 in an unusual environmental condition (NonSPI2) (Fig. 3B-C and Fig. 4B). NonSPI2 media
465 differs from InSPI2 media by having a higher pH (pH7.4 versus pH5.8) and a higher level of
466 phosphate (Löber *et al.*, 2006). This apparent differential expression of SPI2 genes at the
467 transcriptomic level under non-inducing conditions led us to investigate the expression of SPI2
468 at a single cell level using fluorescence transcriptional fusions. First, we introduced an *ssaG*-
469 GFP⁺ transcriptional fusion into the chromosome of strains D33712 and D23580 (Methods;
470 Table S8) to interrogate expression of the key SPI2 operon with flow cytometry. Figure 5B
471 shows that in NonSPI2 media, the *ssaG* promoter was expressed at a 62% higher level in
472 D33712 than in D23580 confirming the results of the transcriptomic analysis.



473

474 **Fig 5. Phenotypes that distinguish ST313 L2.2 from ST313 L2.0. (A)** Swimming motility
475 assay of strains D23589, D37712 and 4/74, with a representative plate shown on the left.
476 Average migration diameters were measured after 4 and 8 hours. Each bar represents the
477 mean of three biological replicates, with error bars representing standard deviation. Significant
478 difference (*** indicates P value (t test) < 0.001). In Panels B & C, comparison of *ssaG*
479 expression by flow cytometry using D23580 and D37712 derivatives containing a chromosomal
480 *ssaG*-GFP⁺ transcriptional fusion, strains Szs008 and Szs032, respectively. Cells were
481 collected at 8 hours after inoculation in NonSPI2 media. Ten thousand events were acquired
482 for each sample. (B) Mean fluorescent intensity signal of *ssaG*-GFP⁺ for D23580 (Szs008, dark
483 grey) and D37712 (Szs032, grey). Significant difference (*** indicates P value (t test) < 0.001).
484 (C) Percentage of positive (green) and negative cells (white) for *ssaG* expression in each
485 sample. Each bar represents the mean of three biological replicates, error bars show standard
486 deviation. Significant difference (*** indicates P value (t test) < 0.001 . (D) Relative fitness of

487 wild-type D23580 and D37712 and their kanamycin resistant derivatives. Bacterial numbers
488 were determined by overnight culture of a 1:1 mixture (wild-type versus Km^R) in NonSPI2 (red),
489 InSPI2 (blue) and LB (black) media. Each bar represents the mean of three biological replicates
490 with error bars representing standard error. *P* values were determined by *t* test (***: *P* < 0.001;
491 **: *P* < 0.01; *: *P* < 0.05; ns: no significance). A competitive index of 1 indicates the equal fitness
492 of two strains, while a number higher than 1 reflects the increased fitness of kanamycin-
493 resistant derivatives.

494

495 Because only a proportion of *S. Typhimurium* cells express certain pathogenicity island-
496 encoded genes during *in vitro* growth (Ackermann *et al.*, 2008; Hautefort *et al.*, 2003), we
497 determined whether the increased level of expression of SPI2 genes (Fig. 4B) was caused by
498 a higher proportion of D37712 cells expressing SPI2 than D23580 cells. Using derivatives of
499 the two strains that carried the *ssaG*-GFP⁺ construct, we determined the numbers of fluorescent
500 and non-fluorescent cells with flow cytometry (Methods). Under non-inducing conditions,
501 slightly more D37712 cells expressed the *ssaG* SPI2 promoter than D23580 cells (65% vs 60%,
502 respectively) (Fig. 5C). However, this small difference did not account for the 62% increased
503 level of non-induced SPI2 expression seen in Fig. 5B.

504 SPI2 expression is controlled by a complex regulatory system that operates at both a negative
505 and positive level, involving silencing via H-NS (Lucchini *et al.*, 2006), activation by SlyA and
506 SsrB (Fass and Groisman, 2009; Walthers *et al.*, 2011) as well as input from OmpR and Fis
507 under non-inducing conditions (Osborne and Coombes, 2011). The reason for the aberrant
508 SPI2 expression in strain D37712 is worthy of further study. Possible explanations include the
509 incomplete silencing of SPI2 transcription or the partial activation of the SPI2 virulence genes
510 under non-inducing growth conditions.

511

512 **Increased fitness of *S. Typhimurium* ST313 sublineage L2.2 compared with L2.0 in 513 minimal media.**

514 It has become increasingly clear that distinct *Salmonella* pathovariants have evolved particular
515 phenotypic properties that confer fitness advantages during infection of particular avian or
516 mammalian hosts (Branchu *et al.*, 2018). Because *S. Typhimurium* ST313 L2.2 appeared to
517 have displaced *S. Typhimurium* ST313 L2.0 in Malawi, we speculated that *S. Typhimurium*
518 ST313 L2.2 might have the competitive edge in some situations. Accordingly, we determined
519 bacterial fitness using a mixed-growth competition assay (Wiser and Lenski, 2015; Lian *et al.*,
520 2023). The competitive index was calculated in three different growth media using pair-wise
521 combinations of strains D37712 and D23580. Two independent approaches were used to
522 phenotypically distinguish the two strains, one based on antibiotic resistance (Fig. 5D) and the
523 other based on fluorescent tagging (Fig. S5).

524 To confirm that strains engineered to be kanamycin-resistant or gentamicin-resistant did not
525 impact on fitness (Methods), we first verified that the tagged variants of D37712 or D23580 did
526 not confer a growth advantage in LB or NonSPI2 media (Fig. S7). Next, we used a mixed-

527 growth assay to investigate fitness of *S. Typhimurium* ST313 L2.0 strain D23580 or *S.*
528 *Typhimurium* ST313 L2.2 strain D37712 during growth in LB, or InSPI2 or NonSPI2 minimal
529 media. The data show that both strains grew at similar levels following overnight mixed-growth
530 in nutrient-rich LB media, but D37712 had a competitive advantage during mixed-growth in
531 InSPI2 media (CI = 1.79; $P<0.05$) and a greater competitive edge in NonSPI2 media (CI = 2.20;
532 $P<0.0001$).

533 We then used an independent fluorescence-based approach to assess the fitness of strains
534 D23580 and D37712 during mixed-growth in NonSPI2 media. This time, the strains were
535 engineered to carry either mScarlet or sGFP2 proteins and the mixed-growth experiments
536 involved pair-wise comparisons of reciprocally-tagged strains. The flow cytometric data showed
537 that in both cases D37712 had a significant competitive advantage in NonSPI2 media (Fig. S5
538 and S6).

539 This combination of antibiotic resistance-based and fluorescence-based competitive index
540 experiments lead us to conclude that *S. Typhimurium* ST313 L2.2 strain D37712 had a clear
541 fitness advantage over *S. Typhimurium* ST313 L2.0 strain D23580 during mixed-growth in two
542 formulations of minimal media. The molecular basis of this fitness advantage remains to be
543 established.

544
545 **Perspective**

546 Here, we report that *S. Typhimurium* ST313 L2.0 has been clonally replaced by the ST313
547 sublineages L2.2 and L2.3 as a cause of bloodstream infection in Blantyre, Malawi. In 2018,
548 L2.2 represented the majority of the ST313 strains isolated from hospitalised patients in Malawi
549 at the Queen Elizabeth Central Hospital. Our comparative genomic analysis of ST313 L2.3
550 identified 30 chromosomal alterations, one of which generated a deletion of the *sseI* effector
551 gene.

552 Our RNA-seq-based analysis of ST313 L2.2 involved a detailed comparison versus ST313 L2.0
553 which revealed a key difference involving SPI2 expression. Following initially observations at
554 the transcriptomic level in the ST313 L2 and L2.2 strains grown in a pH-neutral minimal medium
555 (NonSPI2), the increased expression of SPI2 was confirmed at the single cell level using an
556 *ssaG* transcriptional fusion.

557 A series of experiments showed that the ST313 L2.2 strain D37712 had a competitive
558 advantage over L2 strain D23580 during mixed-growth in minimal media. We propose that this
559 increased fitness of *S. Typhimurium* ST313 L2.2 has contributed to the replacement of ST313
560 L2.0 in Malawi in recent years.

561 Previously, we compared three virulence properties of the *S. Typhimurium* ST313 L2.0 D23580
562 and ST313 L2.2 D37712 strains. First, experiments involving Mucosal Invariant T (MAIT) cells
563 showed that both D37712 and D23580 fail to elicit the high level of activation of MAIT cells that
564 characterises infection by *S. Typhimurium* ST19 4/74 (Preciado-Llanes *et al.*, 2020). Second,

565 the D37712 and D23580 strains stimulate similar levels of up-regulation of IL10 gene
566 expression upon infection of human dendritic cells (Aulicino *et al.*, 2022). Third, we showed that
567 both D37712 and D23580 express similarly high levels of the PgtE virulence factor that is
568 responsible for the ability of *S. Typhimurium* ST313 to survive human serum-killing (Hammarlöf
569 *et al.*, 2018). These findings lead us to conclude that the comparative genomic and
570 transcriptomic differences that distinguish *S. Typhimurium* ST313 L2.0 strain D23580 from
571 ST313 L2.2 D37712 (Fig. 4) do not modulate the ability of the pathogens to activate human
572 MAIT cells or dendritic cells, or to influence the PgtE-mediated serum survival phenotype of *S.*
573 *Typhimurium* ST313.

574 Ideally, the implications of the competitive advantage of ST313 L2.2 would be determined in
575 the context of pathogenesis. However, we lack an informative infection model for *S.*
576 *Typhimurium* ST313 (Lacharme-Lora *et al.*, 2019), and it is not yet possible to experimentally
577 determine whether the improved fitness of L2.2 significantly enhances the success of ST313
578 during infection of humans.

579 Here we have investigated the intricate interplay of gene function that is underpinning the
580 success of *S. Typhimurium* ST313 L2.2. We hope that our findings might contribute to future
581 therapeutic or prophylactic strategies for combatting iNTS infections in the African setting.

582 **Materials and methods**

583 **Bacterial strains**

584 The two *S. Typhimurium* ST313 strains that are the focus of this study are D23580 and D37712.
585 D23580 was isolated from a Malawian 26-month-old child with malaria and anaemia in 2004.
586 D37712 was isolated from the blood of an HIV-positive Malawian male child in 2006. These two
587 African *Salmonella* strains have been deposited in the National Collection of Type Cultures
588 (NCTC). The D23580 (lineage 2.0) strain is available as [NCTC 14677](#). The ST313 sublineage
589 2.2 strain D37712 is available as [NCTC 14678](#). All bacterial strains are detailed in Table S8.

590 **Genome sequencing**

591 The assembled genome and annotation of D23580 (Kingsley *et al.*, 2009; Canals *et al.*, 2019b)
592 (L2.0) was obtained from the European Nucleotide Archive (ENA) repository (EMBL-EBI) under
593 accession PRJEB28511 (<https://www.ebi.ac.uk/ena/data/view/PRJEB28511>). For genome
594 sequencing of D37712 (L2.2), DNA was extracted using the Bioline mini kit, and quality was
595 assessed using gel electrophoresis (0.5% agarose gel, at 30 volts for 18 h). The genome was
596 generated by a combination of long read sequencing with a PacBio RS II and short-read
597 sequencing on an Illumina HiSeq machine at the Center for Genome Research, University of
598 Liverpool, United Kingdom.

599 Sequence reads were quality checked using FastQC version 0.11.9 (Andrews, 2010) and
600 MultiQC version 1.8 (Ewels *et al.*, 2016), trimmed using Trimmomatic (Bolger *et al.*, 2014).
601 Hybrid assembly of the Illumina and PacBio sequence reads was done with Unicycler v0.4.7
602 (Wick *et al.*, 2017).

603 The assembled genome of *S. Typhimurium* ST313 L2.2 strain D37712 was deposited in
604 Genbank (GCA_014250335.1, assembly ASM1425033v1). Raw sequencing reads were
605 deposited for both PacBio and Illumina, under BioProject ID PRJNA656698. Sequence Read
606 Archive (SRA) database IDs are: SRR12444880 for Illumina and SRR12444881 for PacBio.

607 **Comparative genomic analyses**

608 To generate the data summarised in Fig 1C, sequencing data of 29 *S. Typhimurium* ST313
609 strains (Msefula *et al.*, 2012) were downloaded from EMBL-EBI database
610 (<https://www.ebi.ac.uk>, accession number ERA015722). Sequence reads were assembled
611 using Unicycler v0.4.8 (Wick *et al.*, 2017). The quality of the assemblies was assessed by Quast
612 v5.0.2 (Gurevich *et al.*, 2013). The N50 value of all assemblies was >20kb, and the number of
613 contigs was <600.

614 To construct the phylogenetic tree (Fig 1C), *Salmonella* Typhimurium strains D23580, D37712,
615 LT2 (GCA_000006945.2), DT104 (GCA_000493675.1), 4/74 (GCA_000188735.1), and A130
616 (GCA_902500285.1) were added as contextual genomes. Roary was used to make the core
617 gene alignment, construct the gene presence/absence matrix and identify orthologous genes
618 (Page *et al.*, 2015). Phylogenetic trees were constructed using Randomized Accelerated

619 Maximum Likelihood (RAxML) (Stamatakis *et al.*, 2005), and were visualised with the interactive
620 Tree of Life online tool (iTOL) (Letunic and Bork, 2006).

621 The assembled genome and annotation of *S. Typhimurium* ST19 representative strain 4/74
622 (Richardson *et al.*, 2011) were obtained from GenBank (Accession number GCF_000188735.1),
623 while the raw sequencing data of 27 *S. Typhimurium* ST313 strains described in a previous
624 study (Msefula *et al.*, 2012) were downloaded from EMBL-EBI database (<https://www.ebi.ac.uk>,
625 accession number ERA015722). The raw reads were assembled using Unicycler v0.4.8 (Wick
626 *et al.*, 2017). The quality of the assemblies was assessed by Quast v5.0.2 (Gurevich *et al.*,
627 2013). The N50 value of all assemblies was >20kb, and the number of contigs was <600.

628 To identify SNPs, Snippy v4.4.0 (<https://github.com/tseemann/snippy>) was used to map the raw
629 reads against the 4/74 genome. To detect pseudogene-associated SNPs/indels in each sub-
630 lineage, the SNPs/indels that caused nonsense or frameshifted mutations were filtered. The
631 identifications and names of the disrupted genes were summarised, then the wild type gene
632 sequences were extracted from the 4/74 genome. To validate the pseudogene-associated
633 SNPs/indels, the wild type gene sequences were used to make a BLAST database with BLAST
634 2.9.0+ (Camacho *et al.*, 2009). The 29 genome assemblies were queried against the databases,
635 using the BLASTn algorithm to confirm the nonsense and frameshifted mutations in all isolates.

636 **Phylogenetic analysis of African *Salmonella* Typhimurium isolates dating from 1966 -
637 2018**

638 To examine the overall population structure of *Salmonella* Typhimurium responsible for blood
639 infection in Malawi (Fig 1AB and Fig S1), the raw reads of 707 published genome sequences
640 were downloaded (Table S7). Sequence reads were aligned to the *S. Typhimurium* D23580
641 genome using Snippy v4.4.0. The recombination sites of the alignment were removed by
642 Gubbins (Croucher *et al.*, 2015), and the phylogenetic tree was built with Raxml-ng (Kozlov *et*
643 *al.*, 2019). The tree was rooted on *Salmonella* Typhi strain CT18 (GCA_000195995.1) as the
644 outgroup. The tree was visualised with the interactive Tree of Life online tool (iTOL) (Letunic
645 and Bork, 2006). The sub-lineages were identified with rHierBAPS (Tonkin-Hill *et al.*, 2018).
646 The stacked-area chart and the bar chart showing the percentage and number of isolates from
647 each sub-lineage were made in MS Excel.

648 **RNA purification and growth conditions**

649 Initially, a screen of transcriptomic gene expression was performed without biological
650 replicates. Total RNA was purified using TRIzol from *S. Typhimurium* D37712 grown in 15
651 different conditions as described previously (Kröger *et al.*, 2013). To generate statistically-
652 robust gene expression profiles, total RNA was subsequently purified using TRIzol from *S.*
653 *Typhimurium* D37712 grown in four *in vitro* growth conditions (ESP, anaerobic growth,
654 NonSPI2, InSPI2) with three biological replicates as described previously (Kröger *et al.*, 2013).
655 RNA was isolated from intra-macrophage D37712 following infection of RAW264.7 murine
656 macrophages using our published protocol (Srikumar *et al.*, 2015).

657 **RNA-seq of *S. Typhimurium* strain D37712 using Illumina technology**

658 For transcriptomic analyses, cDNA samples were prepared from *S. Typhimurium* RNA by Vertis
659 Biotechnologie AG (Freising, Germany). RNA was first treated with DNase and purified using
660 the Agencourt RNAClean XP kit (Beckman Coulter Genomics). RNA samples were sheared
661 using ultrasound, treated with antarctic phosphatase and re-phosphorylated with T4
662 polynucleotide kinase. RNA fragments were poly(A)-tailed using poly(A) polymerase and an
663 RNA adapter was ligated to the 5'- phosphate of the RNA. First-strand cDNA synthesis was
664 performed using an oligo(dT)-adapter primer and M-MLV reverse transcriptase. The resulting
665 cDNA was PCR-amplified to about 10-20 ng/μl. The cDNA was purified using the Agencourt
666 AMPure XP kit. The cDNA samples were pooled using equimolar amounts and size fractionated
667 in the size range of 200-500 bp using preparative agarose gels. The cDNA pool was sequenced
668 on an Illumina NextSeq 500 system using 75 bp read length.

669 For the biological replicates of the four growth conditions (ESP, anaerobic growth (abbreviated
670 as NoO₂), NonSPI2, and InSPI2) and the intra-macrophage RNA, cDNA samples were
671 generated as above with some improvements in library preparation. First, after fragmentation
672 with ultrasound, an oligonucleotide adapter was ligated to the 3' end of the RNA molecules.
673 Second, first-strand cDNA synthesis was performed using M-MLV reverse transcriptase and
674 the 3' adapter as primer, and, after purification, the 5' Illumina TruSeq sequencing adapter was
675 ligated to the 3' end of the antisense cDNA. Sequencing of the cDNA was performed as
676 described above. All raw sequencing reads were deposited to the Gene Expression Omnibus
677 (GEO) database under accession GSE161403.

678 **RNA-seq and dRNA-seq read processing and visualization**

679 RNA-seq data from *S. Typhimurium* 4/74 and D23580 were extracted from previously published
680 experiments (Kröger *et al.*, 2013; Srikumar *et al.*, 2015; Canals *et al.*, 2019b; GEO dataset
681 GSE119724). A combined reference genome was generated that contained the D23580
682 chromosome plus plasmids pBT1, pBT2, pBT3, pSLT-BT (from D23580) and the D37712
683 plasmid pCol1B9^{D37712}. All reads were aligned and quantified using Bacpipe v0.8a
684 (<https://github.com/apredeus/multi-bacpipe>). Briefly, basic read quality control was performed
685 with FastQC v0.11.8. RNA-seq reads were aligned to the genome sequence using STAR
686 v2.6.0c using “--alignIntronMin 20 --alignIntronMax 19 --outFilterMultimapNmax 20” options. A
687 combined GFF file was generated by Bacpipe, where all features of interest were listed as a
688 “gene”, with each gene identified by a D37712 locus tag. Subsequently, read counting was
689 done by featureCounts v1.6.4, using options “-O -M --fraction -t gene -g ID -s 1”. For
690 visualization, scaled gedGraph files were generated using bedtools genomecov with a scaling
691 coefficient of 10⁹/(number of aligned bases), separately for sense and antisense DNA strands.
692 Bedgraph files were converted to bigWig using bedGraphToBigWig utility
693 (http://hgdownload.soe.ucsc.edu/admin/exe/linux.x86_64/). Coverage tracks, annotation, and
694 genome sequence were visualized using JBrowse v1.16.6. Transcripts Per Million (TPM) were
695 calculated for all samples and used as absolute expression values (Table S5). A conservative

696 cut-off was used to distinguish between expressed (TPM >10) and not expressed (TPM ≤10),
697 as we previously described (Kröger *et al.*, 2013). Relative expression values were calculated
698 by dividing the TPM value for one condition in one strain by the TPM value for the same
699 condition in a different strain. Before the calculation, all TPM values below 10 were set up to
700 10. A conservative fold-change cut-off of 3 was used to highlight differences in expression
701 between strains.

702 **Differential gene expression analysis with multiple biological replicates**

703 For differential expression analysis of *S. Typhimurium* strains 4/74, D23580, and D37712, the
704 raw counts (Table S4) from 3-5 biological replicates in four growth conditions were used (ESP,
705 anaerobic growth (abbreviated as NoO₂), NonSPI2, and InSPI2). Differential expression
706 analysis was done using DESeq2 v1.24.0 with default settings. A gene was considered to be
707 differentially expressed if the absolute value of its log₂ fold change was at least 1 (i.e. fold
708 change > 2), and adjusted p-value was < 0.001.

709 **The SalComD37712 community data resource, and the associated Jbrowse genome
710 browser**

711 SalCom provides a user-friendly Web interface that allows the visualisation and comparison of
712 gene expression values across multiple conditions and between strains. Particular genes can
713 be selected through pre-defined lists of interest, such as all sRNAs or all genes belonging to a
714 specific pathogenicity island. The resulting heatmap-style display highlights expression
715 differences, and provides access to the rich, manually curated annotation of strains D37712
716 and D23580. The actual values behind the display can be downloaded for further processing,
717 and a link connects the current view to a genome browser interface.

718 Visualisation of all the RNA-seq and dRNA-seq (TSS) coverage tracks in JBrowse 1.16.6 shows
719 sequence reads mapped against the combined reference genome described above. Overall,
720 the genomic distance between strains 4/74 and D23580 (approximately 1000 SNPs, or ~1 SNP
721 per 5000 nucleotides), and between D37712 and D23580 (approximately 30 SNPs, ~1 SNP
722 per 150,000 nucleotides) allowed the alignment of RNA-seq reads to the simplified combined
723 reference genome without significant loss of reads. The combined reference genome facilitated
724 a direct comparison of gene coverage as well as transcriptional start sites. The unified browser
725 is hosted at http://hintonlab.com/jbrowse/index.html?data=Combo_D37/data.

726 **Phenotypic and mixed competitive growth experiments**

727 The swimming motility of *S. Typhimurium* strains D37712, D23580 and 4/74 was determined
728 by a plate assay (Canals *et al.*, 2019b), which involved spotting 3 µL overnight culture onto
729 0.3% LB agar. Relative motility of the three strains was assessed by migration diameter after
730 4h and 8h of incubation at 37°C.

731 Relative expression of the *ssaG* SPI2 promoter in strains D23580 and D37712 was measured
732 at the single cell level via GFP fluorescence. Following the construction of a kanamycin-
733 sensitive derivative of D23580 (strain JH4235), a *PssaG::gfp*⁺ transcriptional fusion was

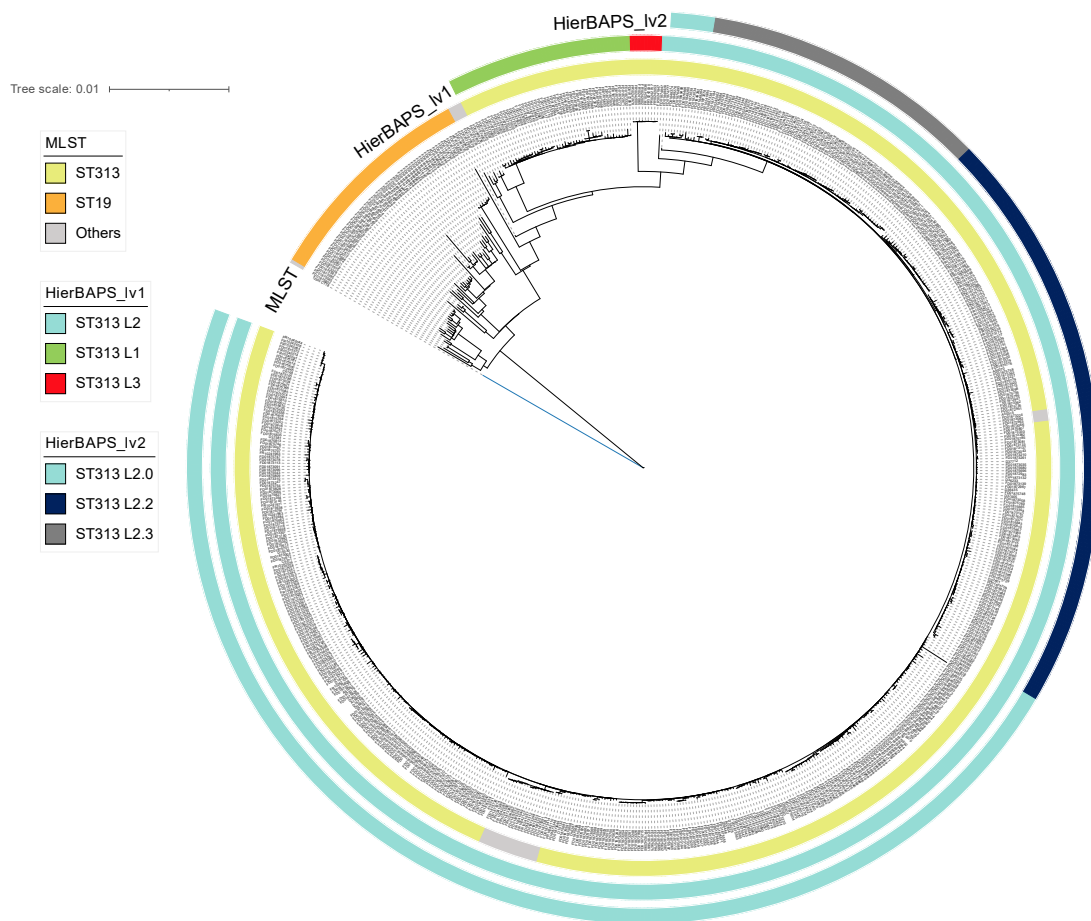
734 incorporated into the chromosome of JH4235 and D37712 by inserting the *gfp*⁺ gene
735 downstream of the *ssaG* gene, under the control of the *PssaG* promoter. The *PssaG::gfp*⁺
736 D23580 derivative (JH4692), and the *PssaG::gfp*⁺ D37712 derivative (JH4693) are listed in
737 Table S8.

738 The strains JH4692 and JH4693 were genome sequenced to confirm the integrity of the
739 transcriptional fusions, and to verify that unintended nucleotide changes had not arisen.
740 Following growth in 25 mL non-inducing NonSPI2 media in a 250 mL flask at 37°C with shaking
741 at 220 rpm for approximately 8 hours until OD₆₀₀=0.3, fluorescence was determined with a BD
742 FACSAria Flow Cytometer. The relative fluorescence of the two strains JH4692 and JH4693,
743 and the numbers of individual fluorescent bacteria that expressed the *PssaG::gfp*⁺ promoter,
744 were determined with FlowJo VX software.

745 The relative fitness of *S. Typhimurium* strains D37712 and D23580 was assessed in two
746 independent mixed-growth experiments. First, kanamycin-resistant derivatives of each strain
747 were constructed by inserting the *aph* kanamycin resistance gene into the chromosome at the
748 intergenic region between the *STM4196* and *STM4197* genes, a region that we have previously
749 shown to be transcriptionally silent (Canals *et al.*, 2019b). The strains were designated
750 D23580::Km^R JH3794 and D37712::Km^R, JH4232. Mixed cultures of wild-type or kanamycin-
751 resistant derivatives of each strain were grown overnight in LB, InSPI2 and NonSPI2 media in
752 a 250 mL flask at 37°C with shaking at 220 rpm. Following plating on LB agar or LB +
753 kanamycin, colonies were counted and the ratio of bacterial strains was determined. To confirm
754 that the insertion of kanamycin resistance at the intergenic region between *STM4196* and
755 *STM4197* did not impact upon fitness, a mixed-growth experiment was done in both LB and
756 NonSPI2 media (Fig. S7).

757 Second, to independently assess relative fitness, Tn7-based plasmids (Schlechter and Remus-
758 Emsermann, 2019) were used to construct chromosomal sGFP2 and mScarlet derivatives of
759 *S. Typhimurium* strains D23580 (sGFP2 derivative: JH4694; mScarlet derivative: JH4695) and
760 D37712 (sGFP2 derivative: JH4696; mScarlet derivative: JH4697). The gene cassettes were
761 inserted into the *S. Typhimurium*Tn7 insertion site between the gene *STMMW_38451* and
762 *glmS*. Mixed cultures of pairs of fluorescently-labelled strains were grown in NonSPI2 media at
763 37°C with shaking at 220 rpm for approximately 8 hours until OD₆₀₀=0.3. Levels of green and
764 red fluorescence were determined with a BD FACSAria Flow Cytometer.

765 **Supporting information**



766

767 **Fig S1, Maximum-likelihood phylogeny of 707 African *S. Typhimurium* isolates.** All
768 genome sequences have been published (Msefula et al., 2012, Pulford et al., 2021, Canals et
769 al., 2019b). Raw sequence reads were aligned to the *S. Typhimurium* D23580 genome
770 (FN424405) using Snippy. The recombination sites of the alignment were removed by Gubbins,
771 and the phylogenetic tree was built with Raxml-ng. The tree is rooted on *Salmonella* Typhi strain
772 CT18 as the outgroup. The MLST sequence types, HierBAPS level 1 and level 2 clusters are
773 shown in coloured concentric rings as indicated. The *S. Typhimurium* ST313 isolates are
774 categorised as Lineage 1, Lineage 2 or Lineage 3 according to HierBAPS level 1 clustering.
775 ST313 Lineage 2 was then sub- divided into 3 sub-lineages according to HierBAPS level 2
776 clustering: ST313 L2.0, ST313 L2.2 and ST313 L2.3. The metadata and lineage designations
777 of all the *S. Typhimurium* isolates are in Table S7.

778

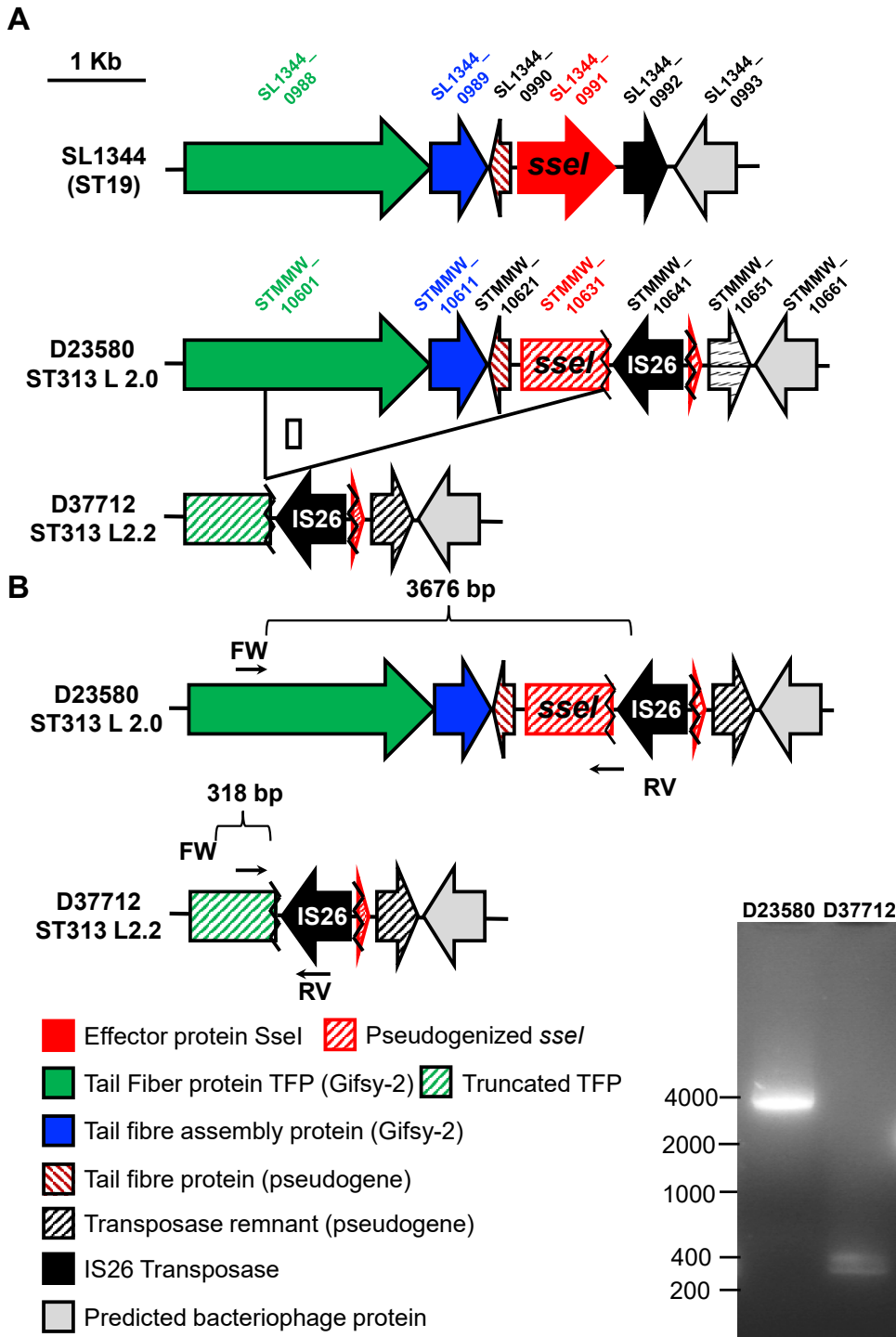
779

780

781

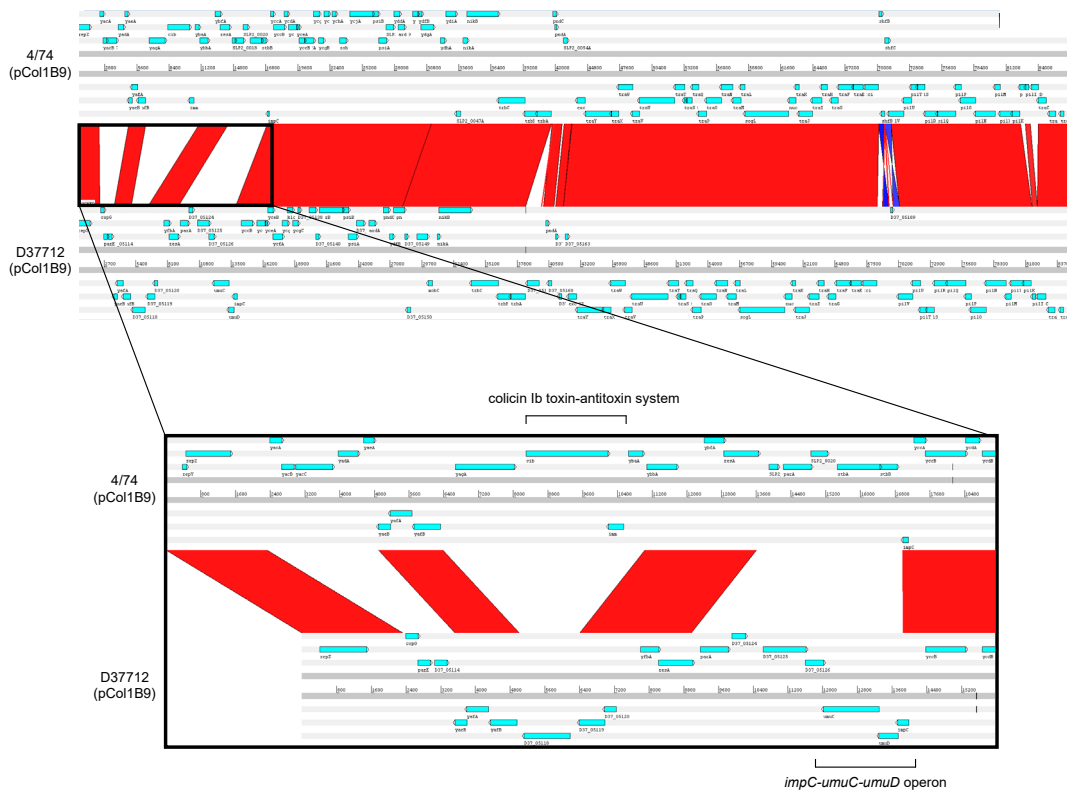
782

783



784

785 **Fig S2.** PCR-based confirmation of the deletion of the *ssel* gene from *S. Typhimurium* L2.2
786 D37712. Arrows from left to right show the forward strand while the left strand is shown by
787 arrows from right to left. However, *ssel* gene in D23580 is a pseudogene with a SNP
788 indicated as a red line.



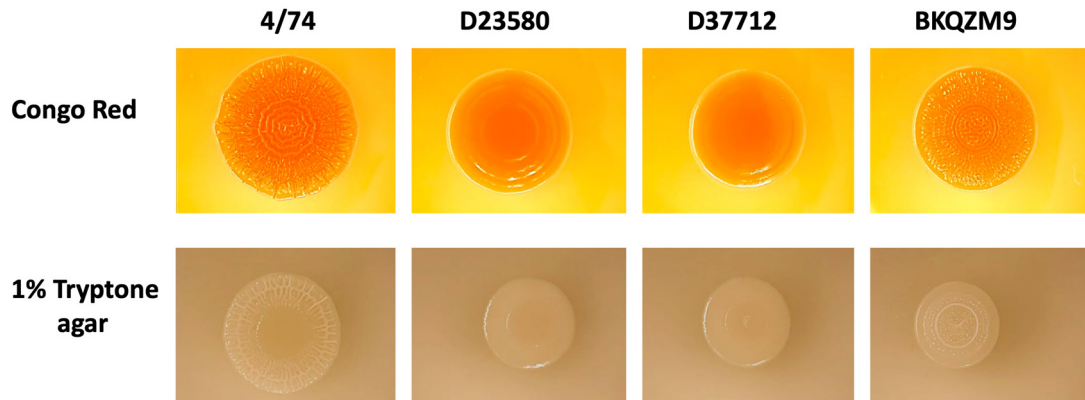
789

790 **Fig S3.** Genomic comparison of plasmids pCol1B9^{4/74} and pCol1B9^{D37712} using Artemis
791 Comparison Tool (ACT). Bottom panel details the differences observed in the most divergent
792 regions, including colicin toxin-antitoxin system (in pCol1B9) and *impC-umuC-umuD* operon (in
793 pCol1B9).

794

795

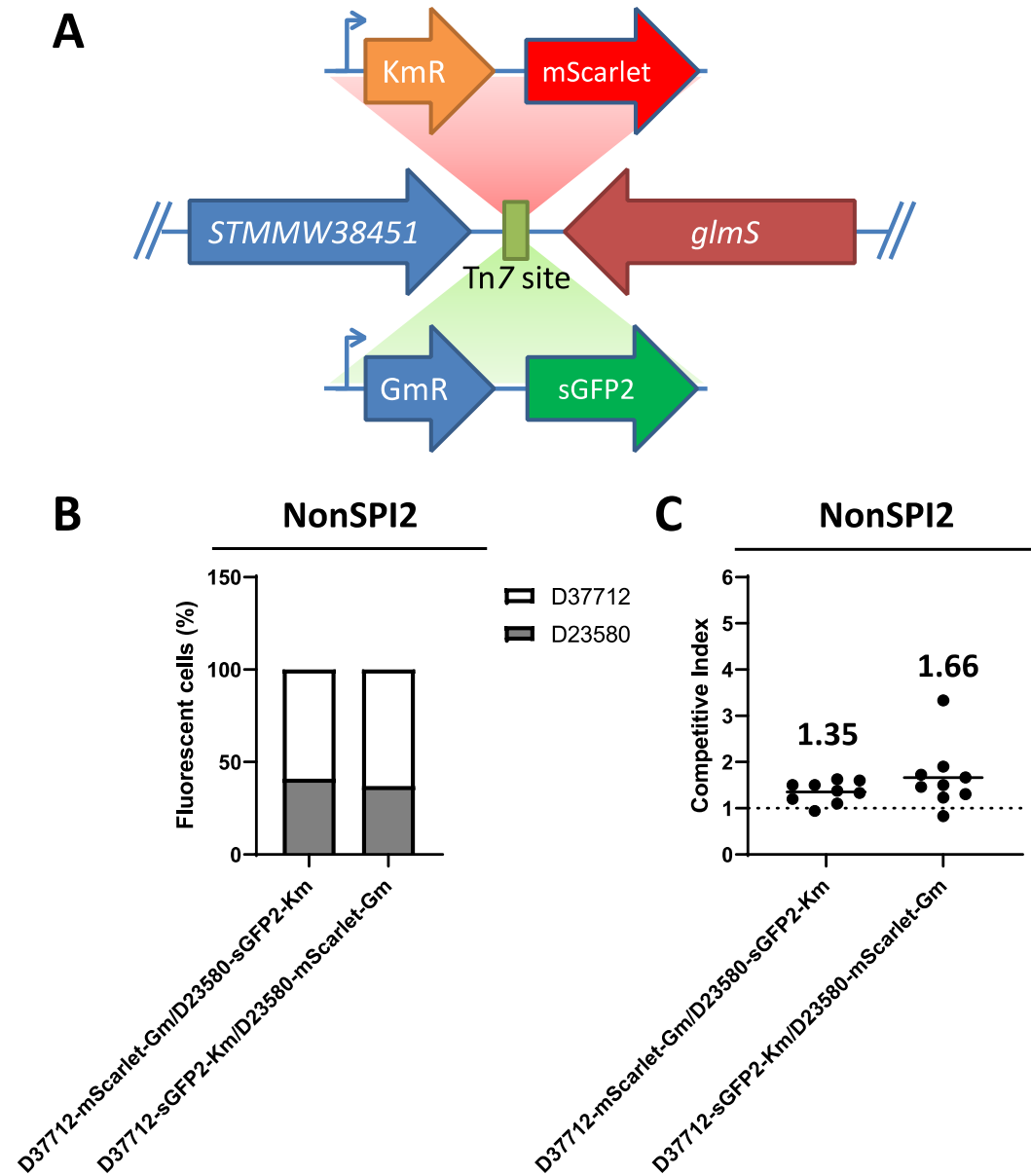
796



797

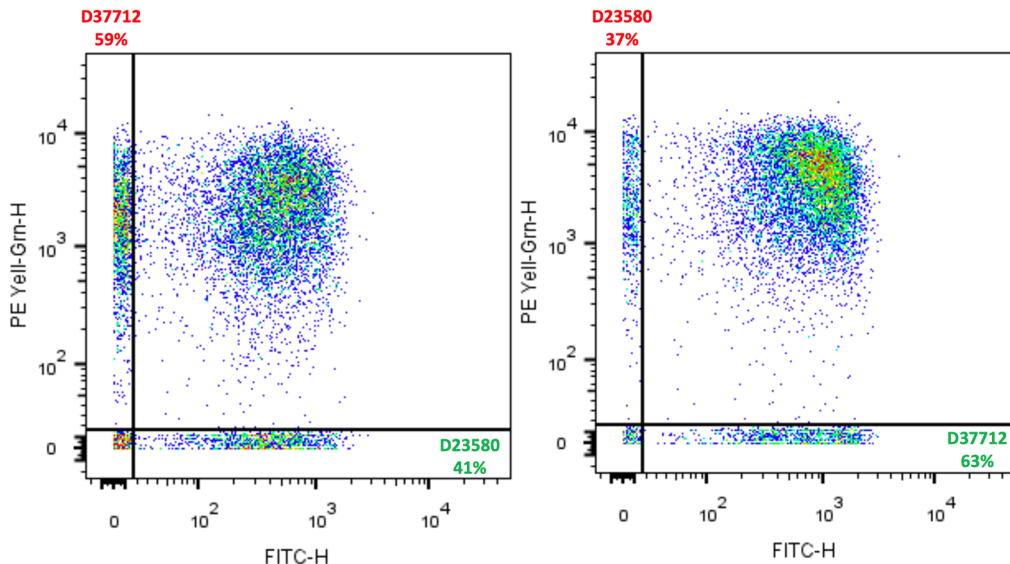
798 **Fig S4. RDAR Phenotypes of 4/74, D23580, D37712 and BKQZM9.** The top panel shows
799 the RDAR morphology assay and the bottom panel shows a complementary experiment that
800 involves the induction of biofilm formation on 1% tryptone agar (MacKenzie et al., 2019).
801 Strain 4/74 was used as a RDAR-positive control, which has concentric rings and a wrinkled
802 appearance (Pulford et al., 2021). The S. Typhimurium ST313 L3 strain BKQZM9 is shown for
803 comparative purposes.

804



805

806 **Fig S5. Competitive index analysis of D23580 and D37712 using fluorescently-tagged *S.***
807 ***Typhimurium* strains (A)** *Km*^R-*sGFP2* and *Gm*^R-*mScarlet* were inserted into the transposon
808 *Tn7* site of D23580 or D37712. Bent arrows represent promoters and directional arrows
809 represent genes. **(B)** A 1:1 mix of *Km*^R-*sGFP2* and *Gm*^R-*mScarlet* marked strain was inoculated
810 in NonSPI2 media, followed by an overnight incubation in 37°C. Percentage of *sGFP2* (green)
811 and *mScarlet* (Red) marked cells was measured by flow cytometry. Raw data are shown in
812 Figure S7, 10,000 events were acquired for each sample. **(C)** Competitive index analysis of
813 *Km*^R-*sGFP2* and *Gm*^R-*mScarlet* marked strain. Bacterial numbers were determined by counting
814 CFU for overnight culture of a 1:1 mixture in NonSPI2 media. Each dot represents a single
815 biological replicate and the lane represents mean value. A competitive index of 1 indicates the
816 equal fitness of two strains, while a number higher than 1 reflects an increased fitness of
817 D37712.



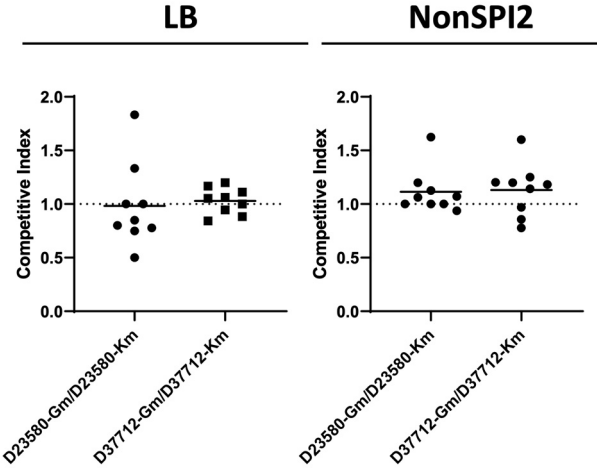
818

819 **Fig S6. Raw flow cytometric data related to Fig. S5B. (A)** JH4695 + JH4698 and **(B)**
820 JH4696 + JH4697. A 1:1 mix of the Km^R-sGFP2 and Gm^R-mScarlet marked strains were
821 inoculated in NonSPI2 media, followed by growth at 37°C until OD₆₀₀ = 0.3. The X-axis
822 (labelled FITC) shows the GFP level and the Y-axis (labelled PE Yell-Grn) indicates the
823 mScarlet level. Quadrant gates were used to separate four populations, and the black
824 numbers indicate the percentage of events in each quadrant. In total, 10,000 events were
825 acquired for each sample.

826

827

828



829

830 **Fig S7. The insertion of GFP-Km or RFP-Gm did not impact on fitness.** A 1:1 mix of Km^R-
831 sGFP2 and Gm^R-mScarlet marked strains were inoculated in LB or NonSPI2 media, followed
832 by overnight incubation in 37°C. The competitive index (CI) was calculated using the formula
833 $(\text{CFU}_{\text{Gm}})/(\text{CFU}_{\text{Km}})$. Each dot represents the CI from a single replicate and the horizontal bars
834 indicate the mean of each dataset.

835

836 **Supplementary data**

837 **Table S1:** SNP and indel variants that differentiate L2.2 (strain D37712) and L2.3 (strain
838 D49679).

839 **Table S2:** SNP and indel variants that differentiate L2.2 (strain D37712) and L2.0 (strain
840 D23580).

841 **Table S3:** Pseudogenes carried by ST19 and ST313 L2.0 and L2.2 (strains 4/74, D23580 and
842 D37712).

843 **Table S4:** Raw read counts for all processed RNA-seq samples shown in Figures 3 and 4
844 (strains 4/74, D23580, and D37712).

845 **Table S5:** TPM values for all processed RNA-seq samples shown in Figures 3 and 4 (strains
846 4/74, D23580, and D37712).

847 **Table S6:** Differential expression analysis using DESeq2 for strains D23580 vs D37712
848 grown in four *in vitro* conditions.

849 **Table S7:** Metadata and lineage designations of the 708 S. Typhimurium isolates used to
850 generate the maximum likelihood phylogeny (Fig. S1).

851 **Table S8:** Bacterial strains used in this study.

852 **Acknowledgements**

853 We are grateful to present and former members of the Hinton laboratory for helpful discussions,
854 and to Paul Loughnane for his expert technical assistance.

855 This work was supported by a Wellcome Trust Investigator award [grant numbers
856 106914/Z/15/Z and 222528/Z/21/Z] to J.C.D.H., and by the Malawi-Liverpool-Wellcome
857 Research Centre Director's Fund. B.K. was funded by an AESA-RISE fellowship from the
858 African Academy of Sciences [Grant Number: RPDF-18-04]. For the purpose of open access,
859 the authors have applied a CC BY public copyright licence to any Author Accepted Manuscript
860 version arising from this submission.

861 **Author contributions**

862 **Conceptualization:** B.K., RH, M.A.G., C.L.M. and J.C.D.H.

863 **Data curation:** B.K., R.C., A.V.P., C.V.P., P.A.

864 **Formal analysis:** B.K., R.C., C.V.P., A.V.P., X.Z., C.K., S.V.O., Y.L., P.A., A.D. and J.C.D.

865 **Funding acquisition:** B.K., R.C., A.V.P., X.Z. and J.C.D.H.

866 **Investigation:** B.K., R.C.A., A.V.P., X.Z. and J.C.D.H.

867 **Methodology:** B.K., R.H., M.A.G., C.L.M. and J.C.D.H.

868 **Project administration:** B.K. and J.C.D.H.

869

870

871

872

873

874

875

876

877

878

879

880 **Resources:** B.K., R.H., M.A.G, C.L.M. and J.C.D.H.
881
882 **Software:** B.K. and A.V.P.
883
884 **Supervision:** M.A.G., C.L.G., C.L.M. and J.C.D.H.
885
886 **Validation:** B.K., R.C., A.V.P., X.Z. and J.C.D.H.
887
888 **Visualization:** B.K., R.C., Y.L., C.V.P., A.V.P. and J.C.D.H.
889
890 **Writing original draft:** B.K., R.C. and J.C.D.H
891
892 **Writing reviews and editing:** B.K., R.C., A.V.P., X.Z., C.K., S.V.O., A.D., R.H., M.G and
893 J.C.D.H.
894
895 **Equal contribution:** Authors B.K., R.C. and A.V.P. made equal contributions to this work.
896

897 **References**

898

899 Ackermann M, Stecher B, Freed N, Songhet P, Hardt W, and Doebeli M (2008)
900 Self-destructive cooperation mediated by phenotypic noise. *454*:987–990.

901 Andrews S (2010) FastQC: a quality control tool for high throughput sequence
902 data. Available online at:
903 <http://www.bioinformatics.babraham.ac.uk/projects/fastqc>.

904 Aulicino A, Antanaviciute A, Frost J, Sousa Geros A, Mellado E, Attar M,
905 Jagielowicz M, Hublitz P, Sinz J, Preciado-Llanes L, Napolitani G, Bowden R,
906 Koohy H, Drakesmith H, and Simmons A (2022) Dual RNA sequencing reveals
907 dendritic cell reprogramming in response to typhoidal *Salmonella* invasion.
908 *Commun Biol* 5:111.

909 Bogomolnaya LM, Santiviago CA, Yang H-J, Baumler AJ, and Andrews-
910 Polymenis HL (2008) ‘Form variation’ of the O12 antigen is critical for
911 persistence of *Salmonella* Typhimurium in the murine intestine. *Mol Microbiol*
912 70:1105–1119.

913 Bolger AM, Lohse M, and Usadel B (2014) Trimmomatic: a flexible trimmer for
914 Illumina sequence data. *Bioinformatics* 30:2114–2120.

915 Branchu P, Bawn M, and Kingsley RA (2018) Genome Variation and Molecular
916 Epidemiology of *Salmonella* enterica Serovar Typhimurium Pathovariants.
917 *Infect Immun* 86:e00079-18.

918 Brink T, Leiss V, Siegert P, Jehle D, Ebner JK, Schwan C, Shymanets A, Wiese
919 S, Nürnberg B, Hensel M, Aktories K, and Orth JHC (2018) *Salmonella*
920 Typhimurium effector Ssel inhibits chemotaxis and increases host cell survival
921 by deamidation of heterotrimeric Gi proteins. *PLOS Pathog* 14:e1007248.

922 Camacho C, Coulouris G, Avagyan V, Ma N, Papadopoulos J, Bealer K, and
923 Madden TL (2009) BLAST+: architecture and applications. *BMC Bioinformatics*
924 10:421.

925 Canals R, Chaudhuri RR, Steiner RE, Owen SV, Quinones-Olvera N, Gordon
926 MA, Baym M, Ibba M, and Hinton JCD (2019) The fitness landscape of the
927 African *Salmonella* Typhimurium ST313 strain D23580 reveals unique
928 properties of the pBT1 plasmid. *PLOS Pathog* 15:e1007948.

929 Canals R, Hammarlöf DL, Kröger C, Owen SV, Fong WY, Lacharme-Lora L,
930 Zhu X, Wenner N, Carden SE, Honeycutt J, Monack DM, Kingsley RA,
931 Brownridge P, Chaudhuri RR, Rowe WPM, Predeus AV, Hokamp K, Gordon
932 MA, and Hinton JCD (2019) Adding function to the genome of African
933 *Salmonella* Typhimurium ST313 strain D23580. *PLOS Biol* 17:e3000059.

934 Carden SE, Walker GT, Honeycutt J, Lugo K, Pham T, Jacobson A, Bouley D,
935 Idoyaga J, Tsolis RM, and Monack D (2017) Pseudogenization of the Secreted

936 Effector Gene *ssel* Confers Rapid Systemic Dissemination of *S. Typhimurium*
937 ST313 within Migratory Dendritic Cells. *Cell Host Microbe* 21:182–194.

938 Chirwa E, Dale, H, Gordon, MA, and Ashton, PM (2023) What is the Source of
939 Infections Causing Invasive Nontyphoidal Salmonella Disease? *Open Forum*
940 *Infect Diseases* February 2023.

941 Crump JA, Sjölund-Karlsson M, Gordon MA, and Parry CM (2015) Epidemiology, Clinical Presentation, Laboratory Diagnosis, Antimicrobial
942 Resistance, and Antimicrobial Management of Invasive *Salmonella* Infections.
943 *Clin Microbiol Rev* 28:901–937.

944 Ewels P, Magnusson M, Lundin S, and Käller M (2016) MultiQC: summarize
945 analysis results for multiple tools and samples in a single report. *Bioinformatics*
946 32:3047–3048.

947 Fass E, and Groisman E (2009) Control of *Salmonella* pathogenicity island-2
948 gene expression. *Curr Opin Microbiol* 12:199–204.

949 Feasey NA, Dougan G, Kingsley RA, Heyderman RS, and Gordon MA (2012) Invasive non-typhoidal salmonella disease: an emerging and neglected tropical
950 disease in Africa. *The Lancet* 379:2489–2499.

951 Feasey NA, Hadfield J, Keddy KH, Dallman TJ, Jacobs J, Deng X, Wigley P,
952 Barquist L, Langridge GC, Feltwell T, Harris SR, Mather AE, Fookes M, Aslett
953 M, Msefula C, Kariuki S, Maclennan CA, Onsare RS, Weill F-X, Le Hello S,
954 Smith AM, McClelland M, Desai P, Parry CM, Cheesbrough J, French N,
955 Campos J, Chabalgoity JA, Betancor L, Hopkins KL, Nair S, Humphrey TJ,
956 Lunguya O, Cogan TA, Tapia MD, Sow SO, Tennant SM, Bornstein K, Levine
957 MM, Lacharme-Lora L, Everett DB, Kingsley RA, Parkhill J, Heyderman RS,
958 Dougan G, Gordon MA, and Thomson NR (2016) Distinct *Salmonella Enteritidis*
959 lineages associated with enterocolitis in high-income settings and invasive
960 disease in low-income settings. *Nat Genet* 48:1211–1217.

961 Gilchrist J, and MacLennan C (2019) Invasive Nontyphoidal *Salmonella*
962 Disease in Africa. *Cell Mol Biol E Coli Salmonella Enterobact*, doi: doi:10.1128/
963 ecosalplus.ESP-0007-2018.

964 Grabe GJ, Zhang Y, Przydacz M, Rolhion N, Yang Y, Pruneda JN, Komander
965 D, Holden DW, and Hare SA (2016) The *Salmonella* Effector SpvD Is a
966 Cysteine Hydrolase with a Serovar-specific Polymorphism Influencing Catalytic
967 Activity, Suppression of Immune Responses, and Bacterial Virulence. *J Biol*
968 *Chem* 291:25853–25863.

969 Gurevich A, Saveliev V, Vyahhi N, and Tesler G (2013) QUAST: quality
970 assessment tool for genome assemblies. *Bioinformatics* 29:1072–1075.

971 Hammarlöf DL, Kröger C, Owen SV, Canals R, Lacharme-Lora L, Wenner N,
972 Schager AE, Wells TJ, Henderson IR, Wigley P, Hokamp K, Feasey NA,
973 Gordon MA, and Hinton JCD (2018) Role of a single noncoding nucleotide in

976 the evolution of an epidemic African clade of *Salmonella*. *Proc Natl Acad Sci*
977 115.

978 Hautefort I, Proen  a MJ, and Hinton JCD (2003) Single-Copy Green
979 Fluorescent Protein Gene Fusions Allow Accurate Measurement of *Salmonella*
980 Gene Expression InVitro and during Infection of Mammalian Cells. *Appl Environ*
981 *Microbiol* 69:7480–7491.

982 Honeycutt JD, Wenner N, Li Y, Brewer SM, Massis LM, Brubaker SW,
983 Chairatana P, Owen SV, Canals R, Hinton JCD, and Monack DM (2020)
984 Genetic variation in the MacAB-TolC efflux pump influences pathogenesis of
985 invasive *Salmonella* isolates from Africa. *PLOS Pathog* 16:e1008763.

986 Jennings E, Thurston TLM, and Holden DW (2017) *Salmonella* SPI-2 Type III
987 Secretion System Effectors: Molecular Mechanisms And Physiological
988 Consequences. *Cell Host Microbe* 22:217–231.

989 Johnson R, and Simon M (1985) Hin-mediated site-specific recombination
990 requires two 26 bp recombination sites and a 60 bp recombinational enhancer.
991 *Cell* 41:781–791.

992 Kariuki S, Revathi G, Kariuki N, Kiuru J, Mwituria J, Muyodi J, Githinji JW,
993 Kagendo D, Munyalo A, and Hart CA (2006) Invasive multidrug-resistant non-
994 typhoidal *Salmonella* infections in Africa: zoonotic or anthroponotic
995 transmission? *J Med Microbiol* 55:585–591.

996 Kasumba IN, Pulford CV, Perez-Sepulveda BM, Sen S, Sayed N, Permal-
997 Booth J, Livio S, Heavens D, Low R, Hall N, Roose A, Powell H, Farag T,
998 Panchalingham S, Berkeley L, Nasrin D, Blackwelder WC, Wu Y, Tamboura B,
999 Sanogo D, Onwuchekwa U, Sow SO, Ochieng JB, Omore R, Oundo JO,
1000 Breiman RF, Mintz ED, O'Reilly CE, Antonio M, Saha D, Hossain MJ,
1001 Mandomando I, Bassat Q, Alonso PL, Ramamurthy T, Sur D, Qureshi S, Zaidi
1002 AKM, Hossain A, Faruque ASG, Nataro JP, Kotloff KL, Levine MM, Hinton JCD,
1003 and Tennant SM (2021) Characteristics of *Salmonella* Recovered From Stools
1004 of Children Enrolled in the Global Enteric Multicenter Study. *Clin Infect Dis*
1005 73:631–641.

1006 Kingsley RA, Msefula CL, Thomson NR, Kariuki S, Holt KE, Gordon MA, Harris
1007 D, Clarke L, Whitehead S, Sangal V, Marsh K, Achtman M, Molyneux ME,
1008 Cormican M, Parkhill J, MacLennan CA, Heyderman RS, and Dougan G (2009)
1009 Epidemic multiple drug resistant *Salmonella* Typhimurium causing invasive
1010 disease in sub-Saharan Africa have a distinct genotype. *Genome Res* 19:2279–
1011 2287.

1012 Kirk MD, Pires SM, Black RE, Caipo M, Crump JA, Devleesschauwer B, D  pfer
1013 D, Fazil A, Fischer-Walker CL, Hald T, Hall AJ, Keddy KH, Lake RJ, Lanata CF,
1014 Torgerson PR, Havelaar AH, and Angulo FJ (2015) World Health Organization
1015 Estimates of the Global and Regional Disease Burden of 22 Foodborne
1016 Bacterial, Protozoal, and Viral Diseases, 2010: A Data Synthesis. *PLOS Med*
1017 12:e1001921.

1018 Koolman L, Prakash R, Diness Y, Msefula C, Nyirenda TS, Olgemoeller F,
1019 Perez-Sepulveda B, Hinton JCD, Owen SV, Feasey NA, Ashton PM, and
1020 Gordon MA (2022) *Case-control investigation of invasive *Salmonella* disease*
1021 *in Africa – comparison of human, animal and household environmental isolates*
1022 *find no evidence of environmental or animal reservoirs of invasive strains*,
1023 *Infectious Diseases (except HIV/AIDS)*.

1024 Kröger C, Colgan A, Srikumar S, Händler K, Sivasankaran SK, Hammarlöf DL,
1025 Canals R, Grissom JE, Conway T, Hokamp K, and Hinton JCD (2013) An
1026 Infection-Relevant Transcriptomic Compendium for *Salmonella enterica*
1027 Serovar Typhimurium. *Cell Host Microbe* 14:683–695.

1028 Kröger C, Dillon SC, Cameron ADS, Papenfort K, Sivasankaran SK, Hokamp
1029 K, Chao Y, Sittka A, Hébrard M, Händler K, Colgan A, Leekitcharoenphon P,
1030 Langridge GC, Lohan AJ, Loftus B, Lucchini S, Ussery DW, Dorman CJ,
1031 Thomson NR, Vogel J, and Hinton JCD (2012) The transcriptional landscape
1032 and small RNAs of *Salmonella enterica* serovar Typhimurium. *Proc Natl Acad
1033 Sci* 109.

1034 Lai MA, Quarles EK, López-Yglesias AH, Zhao X, Hajjar AM, and Smith KD
1035 (2013) Innate Immune Detection of Flagellin Positively and Negatively
1036 Regulates *Salmonella* Infection. *PLoS ONE* 8:e72047.

1037 Letunic I, and Bork P (2006) Interactive Tree Of Life (iTOL): an online tool for
1038 phylogenetic tree display and annotation. *Bioinformatics* 23:1283–1287.

1039 Lian ZJ, Phan M, Hancock SJ, Nhu NTK, Paterson DL, and Schembri MA
1040 (2023) Genetic basis of I-complex plasmid stability and conjugation. *PLOS
1041 Genet* 19:e1010773.

1042 Löber S, Jäckel D, Kaiser N, and Hensel M (2006) Regulation of *Salmonella*
1043 pathogenicity island 2 genes by independent environmental signals. *Int J Med
1044 Microbiol* 296:435–447.

1045 Lucchini S, Rowley G, Goldberg MD, Hurd D, Harrison M, and Hinton JCD
1046 (2006) H-NS Mediates the Silencing of Laterally Acquired Genes in Bacteria.
1047 *PLoS Pathog* 2:e81.

1048 Majowicz SE, Musto J, Scallan E, Angulo FJ, Kirk M, O'Brien SJ, Jones TF,
1049 Fazil A, and Hoekstra RM (2010) The Global Burden of Nontyphoidal
1050 *Salmonella* Gastroenteritis. *Clin Infect Dis* 50:882–889.

1051 Marchello C, Dale, A. P., Pisharody, S., Rubach, M. P., and Crump, J.A. (2019)
1052 A Systematic Review and Meta-analysis of the Prevalence of Community-
1053 Onset Bloodstream Infections among Hospitalized Patients in Africa and Asia.
1054 *Antimicrobial Agents and Chemotherapy*. 64.

1055 Marchello CS, Dale AP, Pisharody S, Rubach MP, and Crump JA (2019) A
1056 Systematic Review and Meta-analysis of the Prevalence of Community-Onset
1057 Bloodstream Infections among Hospitalized Patients in Africa and Asia.
1058 *Antimicrob Agents Chemother* 64:e01974-19.

1059 Msefula CL, Kingsley RA, Gordon MA, Molyneux E, Molyneux ME, MacLennan
1060 CA, Dougan G, and Heyderman RS (2012) Genotypic Homogeneity of
1061 Multidrug Resistant *S. Typhimurium* Infecting Distinct Adult and Childhood
1062 Susceptibility Groups in Blantyre, Malawi. *PLoS ONE* 7:e42085.

1063 Musicha P, Cornick JE, Bar-Zeev N, French N, Masesa C, Denis B, Kennedy
1064 N, Mallewa J, Gordon MA, Msefula CL, Heyderman RS, Everett DB, and
1065 Feasey NA (2017) Trends in antimicrobial resistance in bloodstream infection
1066 isolates at a large urban hospital in Malawi (1998–2016): a surveillance study.
1067 *Lancet Infect Dis* 17:1042–1052.

1068 Nedialkova LP, Denzler R, Koeppel MB, Diehl M, Ring D, Wille T, Gerlach RG,
1069 and Stecher B (2014) Inflammation Fuels Colicin Ib-Dependent Competition of
1070 *Salmonella* Serovar *Typhimurium* and *E. coli* in Enterobacterial Blooms. *PLoS*
1071 *Pathog* 10:e1003844.

1072 Okoro CK, Barquist L, Connor TR, Harris SR, Clare S, Stevens MP, Arends MJ,
1073 Hale C, Kane L, Pickard DJ, Hill J, Harcourt K, Parkhill J, Dougan G, and
1074 Kingsley RA (2015) Signatures of Adaptation in Human Invasive *Salmonella*
1075 *Typhimurium* ST313 Populations from Sub-Saharan Africa. *PLoS Negl Trop Dis*
1076 9:e0003611.

1077 Okoro CK, Kingsley RA, Connor TR, Harris SR, Parry CM, Al-Mashhadani MN,
1078 Kariuki S, Msefula CL, Gordon MA, de Pinna E, Wain J, Heyderman RS, Obaro
1079 S, Alonso PL, Mandomando I, MacLennan CA, Tapia MD, Levine MM, Tennant
1080 SM, Parkhill J, and Dougan G (2012) Intracontinental spread of human invasive
1081 *Salmonella* *Typhimurium* pathovariants in sub-Saharan Africa. *Nat Genet*
1082 44:1215–1221.

1083 Owen SV, Wenner N, Canals R, Makumi A, Hammarlöf DL, Gordon MA,
1084 Aertsen A, Feasey NA, and Hinton JCD (2017) Characterization of the
1085 Prophage Repertoire of African *Salmonella* *Typhimurium* ST313 Reveals High
1086 Levels of Spontaneous Induction of Novel Phage BTP1. *Front Microbiol* 8.

1087 Page AJ, Cummins CA, Hunt M, Wong VK, Reuter S, Holden MTG, Fookes M,
1088 Falush D, Keane JA, and Parkhill J (2015) Roary: rapid large-scale prokaryote
1089 pan genome analysis. *Bioinformatics* 31:3691–3693.

1090 Perez-Sepulveda BM, and Hinton JCD (2018) Functional Transcriptomics for
1091 Bacterial Gene Detectives. *Microbiol Spectr* 6:6.5.06.

1092 Piccini G, and Montomoli E (2020) Pathogenic signature of invasive non-
1093 typhoidal *Salmonella* in Africa: implications for vaccine development. *Hum*
1094 *Vaccines Immunother* 16:2056–2071.

1095 Post AS, Diallo SN, Guiraud I, Lombo P, Tahita MC, Maltha J, Van Puyvelde S,
1096 Mattheus W, Ley B, Thriemer K, Rouamba E, Derra K, Deborggraeve S, Tinto
1097 H, and Jacobs J (2019) Supporting evidence for a human reservoir of invasive
1098 non-Typhoidal *Salmonella* from household samples in Burkina Faso. *PLoS*
1099 *Negl Trop Dis* 13:e0007782.

1100 Preciado-Llanes L, Aulicino A, Canals R, Moynihan PJ, Zhu X, Jambo N,
1101 Nyirenda TS, Kadwala I, Sousa Gerós A, Owen SV, Jambo KC, Kumwenda B,
1102 Veerapen N, Besra GS, Gordon MA, Hinton JCD, Napolitani G, Salio M, and
1103 Simmons A (2020) Evasion of MAIT cell recognition by the African *Salmonella*
1104 Typhimurium ST313 pathovar that causes invasive disease. *Proc Natl Acad Sci*
1105 117:20717–20728.

1106 Pulford CV, Perez-Sepulveda BM, Canals R, Bevington JA, Bengtsson RJ,
1107 Wenner N, Rodwell EV, Kumwenda B, Zhu X, Bennett RJ, Stenhouse GE,
1108 Malaka De Silva P, Webster HJ, Bengoechea JA, Dumigan A, Tran-Dien A,
1109 Prakash R, Banda HC, Alufandika L, Mautanga MP, Bowers-Barnard A,
1110 Beliavskia AY, Predeus AV, Rowe WPM, Darby AC, Hall N, Weill F-X, Gordon
1111 MA, Feasey NA, Baker KS, and Hinton JCD (2021) Stepwise evolution of
1112 *Salmonella* Typhimurium ST313 causing bloodstream infection in Africa. *Nat*
1113 *Microbiol* 6:327–338.

1114 Rankin, J.D. and Taylor R.J. (1966) The estimation of doses of *Salmonella*
1115 typhimurium suitable for the experimental production of disease in calves. *Vec*
1116 *Rec* 78:706–7.

1117 Richardson EJ, Limaye B, Inamdar H, Datta A, Manjari KS, Pullinger GD,
1118 Thomson NR, Joshi RR, Watson M, and Stevens MP (2011) Genome
1119 Sequences of *Salmonella enterica* Serovar Typhimurium, Choleraesuis, Dublin,
1120 and Gallinarum Strains of Well- Defined Virulence in Food-Producing Animals.
1121 *J Bacteriol* 193:3162–3163.

1122 Schlechter R, and Remus-Emsermann M (2019) Delivering "Chromatic
1123 Bacteria" Fluorescent Protein Tags to Proteobacteria Using Conjugation.
1124 *BIO-Protoc* 9.

1125 Sikand A, Jaszczur M, Bloom LB, Woodgate R, Cox MM, and Goodman MF
1126 (2021) The SOS Error-Prone DNA Polymerase V Mutasome and β -Sliding
1127 Clamp Acting in Concert on Undamaged DNA and during Translesion
1128 Synthesis. *Cells* 10:1083.

1129 Sri Kumar S, Kröger C, Hébrard M, Colgan A, Owen SV, Sivasankaran SK,
1130 Cameron ADS, Hokamp K, and Hinton JCD (2015) RNA-seq Brings New
1131 Insights to the Intra-Macrophage Transcriptome of *Salmonella* Typhimurium.
1132 *PLOS Pathog* 11:e1005262.

1133 Stamatakis A, Ludwig T, and Meier H (2005) RAxML-III: a fast program for
1134 maximum likelihood-based inference of large phylogenetic trees. *Bioinformatics*
1135 21:456–463.

1136 Stanaway JD, Parisi A, Sarkar K, Blacker BF, Reiner RC, Hay SI, Nixon MR,
1137 Dolecek C, James SL, Mokdad AH, Abebe G, Ahmadian E, Alahdab F,
1138 Alemnew BTT, Alipour V, Allah Bakeshei F, Animut MD, Ansari F, Arabloo J,
1139 Asfaw ET, Bagherzadeh M, Bassat Q, Belayneh YMM, Carvalho F, Daryani A,
1140 Demeke FM, Demis ABB, Dubey M, Duken EE, Dunachie SJ, Eftekhari A,
1141 Fernandes E, Fouladi Fard R, Gedefaw GA, Geta B, Gibney KB, Hasanzadeh
1142 A, Hoang CL, Kasaeian A, Khater A, Kidanemariam ZT, Lakew AM,

1143 Malekzadeh R, Melese A, Mengistu DT, Mestrovic T, Miazgowski B,
1144 Mohammad KA, Mohammadian M, Mohammadian-Hafshejani A, Nguyen CT,
1145 Nguyen LH, Nguyen SH, Nirayo YL, Olagunju AT, Olagunju TO, Pourjafar H,
1146 Qorbani M, Rabiee M, Rabiee N, Rafay A, Rezapour A, Samy AM, Sepanlou
1147 SG, Shaikh MA, Sharif M, Shigematsu M, Tessema B, Tran BX, Ullah I, Yimer
1148 EM, Zaidi Z, Murray CJL, and Crump JA (2019) The global burden of non-
1149 typhoidal salmonella invasive disease: a systematic analysis for the Global
1150 Burden of Disease Study 2017. *Lancet Infect Dis* 19:1312–1324.

1151 Tack B, Phoba M-F, Barbé B, Kalonji LM, Hardy L, Van Puyvelde S, Ingelbeen
1152 B, Falay D, Ngonda D, van der Sande MAB, Deborggraeve S, Jacobs J, and
1153 Lunguya O (2020) Non-typhoidal Salmonella bloodstream infections in Kisantu,
1154 DR Congo: Emergence of O5-negative *Salmonella Typhimurium* and extensive
1155 drug resistance. *PLoS Negl Trop Dis* 14:e0008121.

1156 Van Puyvelde S, Pickard D, Vandelannoote K, Heinz E, Barbé B, de Block T,
1157 Clare S, Coomber EL, Harcourt K, Sridhar S, Lees EA, Wheeler NE, Klemm
1158 EJ, Kuijpers L, Mbuyi Kalonji L, Phoba M-F, Falay D, Ngbonda D, Lunguya O,
1159 Jacobs J, Dougan G, and Deborggraeve S (2019) An African *Salmonella*
1160 *Typhimurium* ST313 sublineage with extensive drug-resistance and signatures
1161 of host adaptation. *Nat Commun* 10:4280.

1162 Wick RR, Judd LM, Gorrie CL, and Holt KE (2017) Unicycler: Resolving
1163 bacterial genome assemblies from short and long sequencing reads. *PLOS*
1164 *Comput Biol* 13:e1005595.

1165 Zhang S, Kingsley RA, Santos RL, Andrews-Polymenis H, Raffatellu M,
1166 Figueiredo J, Nunes J, Tsolis RM, Adams LG, and Bäumler AJ (2003)
1167 Molecular Pathogenesis of *Salmonella enterica* Serotype Typhimurium-
1168 Induced Diarrhea. *Infect Immun* 71:1–12.

1169